UCLA
UCLA Electronic Theses and Dissertations

Title

The Administration of Intranasal Live Attenuated Influenza Vaccine Induces Changes in the Nasal Microbiota and Nasal Epithelium Gene Expression Profile

Permalink

https://escholarship.org/uc/item/7s65s4xj

Author

Tarabichi, Yasir

Publication Date

2015

Peer reviewed|Thesis/dissertation

UNIVERSITY OF CALIFORNIA

Los Angeles

The Administration of Intranasal Live Attenuated Influenza Vaccine Induces Changes in

the Nasal Microbiota and Nasal Epithelium Gene Expression Profile

A thesis submitted in partial satisfaction of the requirements for the degree of Master of

Science in Clinical Research

by

Yasir Tarabichi

2015

ABSTRACT OF THE THESIS

The Administration of Intranasal Live Attenuated Influenza Vaccine Induces Changes in

the Nasal Microbiota and Nasal Epithelium Gene Expression Profile

by

Yasir Tarabichi

Master of Science in Clinical Research

University of California, Los Angeles, 2015

Professor James O. Lloyd-Smith, Chair

Viral infections such as influenza have been shown to predispose hosts to increased

colonization of the respiratory tract by pathogenic bacteria and secondary bacterial

pneumonia. To examine how viral infections and host antiviral immune responses alter

the upper respiratory microbiome, we analyzed the nasal bacterial composition in

healthy volunteers at baseline, 1-2 weeks, and 4-6 weeks after instillation of a live

attenuated influenza vaccine or intranasal sterile saline. In parallel, we also assessed

changes in the nasal microbiome over similar time points in patients presenting with flu-

like illness in ambulatory settings. All samples were subjected to 16S rRNA gene

sequencing for assessment of the microbiota, while a subset of samples from

vaccinated subjects was submitted for microarray host gene expression profiling. We

found that live attenuated influenza vaccination led to significant changes in microbial

community structure, diversity and core taxonomic membership as well as increases in

the relative abundances of *Staphylococcus* and *Bacteroides* (both p<0.05). Hypergeometric testing for the enrichment of gene ontology terms in the vaccinated group reflected a robust up-regulation of type I and type II interferon stimulated genes in the vaccinated group relative to controls. Translational murine studies showed that poly I:C administration did in fact permit greater nasal *Staphylococcus aureus* persistence, a response absent in interferon alpha/beta receptor deficient mice. Collectively, our findings demonstrate that although the human nasopharyngeal bacterial community is heterogeneous and typically individually robust, activation of an antiviral immune response may foster the disproportionate emergence of potentially pathogenic species such as *S. aureus*.

The thesis of Yasir Tarabichi is approved.

Jane C. Deng

Katrina M. Dipple

David Elashoff

James O. Lloyd-Smith, Committee Chair

University of California, Los Angeles

2015

Dedicated to my loving wife, Yosra.

TABLE OF CONTENTS

The Administration of Intranasal Live Attenuated Influenza Vaccine Induces Changes in the Nasal Microbiota and Nasal Epithelium Gene Expression Profiles.

Y. Tarabichi*[1], K. Li*[5], S. Hu*[1], C. Nguyen[3], X. Wang[3], D. Elashoff[3], K. Saira[4$], Bryan Frank[5], Monika Bihan[5], E. Ghedin[4,6], B.A. Methé*[5], J.C. Deng*[1]

[1]Division of Pulmonary and Critical Care Medicine/Department of Medicine; [2]Department of Medicine; [3] Department of Medicine Statistics Core, UCLA, Los Angeles, CA; [4]Department of Computational & Systems Biology, University of Pittsburgh School of Medicine, Pittsburgh, PA; [5]Departments of Human Genome Medicine and Microbial and Environmental Genomics, J. Craig Venter Institute, Rockville, MD; [6]Department of Biology, Center for Genomics & Systems Biology, Global Institute of Public Health, New York University, New York, NY

*equal contribution

INTRODUCTION:

Secondary bacterial pneumonia has been implicated as the main cause of death during influenza pandemics, including the 1918 "Spanish" and 2009 novel H1N1 influenza A virus pandemics (1-3). The worldwide death toll was estimated to be around 50 million in 1918 and 284,400 in 2009 (4, 5). Even in countries with advanced medical systems, bacterial co-infection remained a component of as many as 30% of cases of H1N1 infection (6), evident in 29% of post-autopsy lungs in one series (3). The organisms identified were predominantly *Staphylococcus* and *Streptococcus* species, with relatively higher proportions of *Streptococcus pneumoniae* and *Staphylococcus aureus* specifically (3, 6, 7).

While the lower respiratory tract had classically been considered sterile, there is growing evidence that it harbors its own microbiota (8, 9) and that this niche is informed to a large extent by the contents of the nasopharyngeal compartment (10-12). Colonization of the nares and pharynx with pathogenic bacteria appears to be an essential precursor to lower respiratory tract and other invasive bacterial infections or co-infection (13-17). In murine systems, colonization by potentially pathogenic bacteria such as *S. pneumoniae* also appears to be enhanced in the presence of type I interferon (IFN) (18). Murine models have demonstrated that both type I and type II IFN-mediated host responses to influenza infection act to critically suppress the antibacterial response against pulmonary infection by both *S. pneumoniae* and *S. aureus* (19-25). Whether similar alterations in nasal colonization patterns during viral infections occur in human beings was unknown. Presumably, such a virally mediated change may permit the emergence or overgrowth of potentially pathogenic bacteria as a precursor to

secondary bacterial infection. Further understanding of such a process would be essential towards the development of new interventions or preventative modalities that might depend on tempering the adverse changes in the nasal microbiome and/or host response.

We therefore addressed two questions in this study: We examined (1) how a new viral stimulus affected the upper respiratory tract microbiome, and (2) whether any associations existed between the host immune response to the intranasal live attenuated vaccine (LAIV) and changes in bacterial composition. This nasal spray contains live, weakened viruses that can only grow in the lower temperature of the nasal passage and cannot grow at normal body temperature. LAIV is designed to induce an immune response that mimics the one generated by live influenza (26).

To determine how the nasal microbiome changes during the acute, early recovery and late recovery periods after viral perturbation, we analyzed serial nasal samples from healthy volunteers who were experimentally inoculated with LAIV as well as outpatients presenting to the clinic with acute flu-like illness. In order to examine potential host interactions in the setting of viral perturbation, we profiled host gene expression by microarray analysis after LAIV administration with a focus on type I and type II interferon stimulated genes. Since *Staphylococcus* emerged as one of the genera whose relative abundance increased following LAIV administration, we then validated our observations with a murine model looking at the association between interferon induction and nasal persistence of *S. aureus*.

RESULTS:

Volunteer characteristics and samples analyzed.

*For the interventional portion of the study, we recruited healthy adult subjects who were randomized to receive either nasal LAIV or sterile nasal saline spray. Their nares were sampled at baseline (visit 1), 1-2 weeks (visit 2), and 4-6 weeks (visit 3) after intervention. A total of 17 volunteers completed all three visits of the study, with 10 volunteers administered LAIV (EX group) and 7 receiving saline nasal spray (HV group). The baseline characteristics of these volunteers are presented in **Table 1**. Both groups were comparable in age and gender distribution. Most subjects reported either weekly or daily nose-picking, which has been associated with S. aureus nasal carriage (27).*

*We also recruited adults who presented as outpatients to our emergency department or general internal medicine clinics with flu-like illness, which we defined as having fever and symptoms of upper respiratory illness. Their characteristics are listed in **Table 2**. We obtained serial samples during acute viral illness (visit 1), 1-2 weeks later (visit 2), and at 6-8 weeks after the initial presentation (visit 3). Nasal wash specimens were obtained and sent for respiratory viral panel testing by PCR to detect community acquired respiratory viral infection. Out of 16 total subjects recruited with suspected respiratory viral illness, 6 tested positive for influenza A. An additional 2 had coronavirus detected, while the remainder tested negative.*

Changes in nasal diversity following LAIV versus saline administration.

To determine how the diversity of the nasal microbiome changes following intranasal influenza vaccine (EX) in comparison to the microbiome of volunteers having received

only the nasal saline spray (HV), we obtained serial nasal samples and sequenced hypervariable regions of the 16S rRNA gene amplified from the isolated bacterial DNA. We aimed for a minimum of 5,000 high quality sequence reads per sample for each of the hypervariable regions sequenced, a value achieved in all of the samples submitted for region V3-V5 (34) and all but one of the samples submitted for region V1-V3 analysis (33). In general, the V3-V5 primers resulted in the identification of more taxonomic units when compared to the V1-V3 primers (data not shown), particularly in the groups receiving nasal influenza vaccine. As a result, we focused all EX and HV group analyses on sequencing from V3-V5 regions. At the genus level, taxonomic diversity was measured with the Shannon and Tail (t) statistic (28) diversity indices, the latter being a more sensitive measure of diversity in low abundance taxa. Both the Tail statistic and the Shannon index demonstrated statistically significant within subject differences over time by two-way, repeated measures ANOVA (p=0.047 and p=0.032 respectively). Subsequent Wilcoxon-signed rank testing without correction for multiple testing revealed significant changes in both measures between the first and second visits and the second and third visits in the EX group specifically, but not the HV group **(Figure 1).**

Differences in community structure following LAIV versus saline administration.

We next sought to determine whether the community structures of the individual groups did in fact change over time. In order to quantitatively represent these differences while accounting for inter-subject variability, we conducted a permutational multivariate analysis of variance (PERMANOVA) based on Bray-Curtis dissimilarities

5

between all samples, stratified by subject. The interaction between the intervention (EX versus HV) and time proved significant (p = 0.032), with a medium effect (R^2 = 0.17). To study these potential differences within the individual groups, PERMANOVA was repeated for each group over the first two time-points, when treatment-induced effects were predicted to be the greatest. The HV group showed no significant changes in community structure over time, while the EX group changed significantly (p = 0.006, R^2 = 0.10). These relationships were visually demonstrated by multidimensional scaling (MDS) plots based on the same dissimilarity measures **(Figure 2)**.

Analysis of the microbiome of patients with influenza or flu-like illness.

To determine how the nasal microbiome changes during the acute, early recovery, and late recovery periods after onset of a community acquired respiratory viral illness, we obtained serial nasal samples from outpatients presenting to the clinic or our emergency department with acute flu-like illness. Analysis of the samples from the flu-like illness group (FL) was performed on V1-V3 data, for which we had the most complete sequencing. Only 3 of 57 samples submitted were of insufficient quality to be analyzed. Given that it was not feasible to obtain a true baseline sample (i.e., pre-illness) in the FL group, direct temporal comparisons with the HV or EX groups could not be made; hence, the visit 1 samples obtained at initial presentation of respiratory infection symptoms (when the effect was predicted to be the largest) were compared to subsequent samples within the FL group. On the whole, the FL group showed no significant changes in diversity measures (by Shannon index or Tail statistic) over time (data not shown). PERMANOVA based on Bray-Curtis dissimilarities between all three

6

visits demonstrated statistically significant changes, albeit with a small effect size (p = 0.036, R^2 = 0.033). Applying the PERMANOVA analysis to the first and second visits demonstrated relatively small (R^2=0.044) but statistically significant changes (p = 0.011) **(Figure 3A)**. Analysis of the subset of patients who tested positive for influenza A infection revealed that the effect increased to a medium size (R^2=0.12) (**Figure 3B**). In general, the small effect sizes discovered are not surprising given considerable heterogeneity in the FL group with regards to age and ethnic makeup, as well as the type and severity of viral infection and the duration of symptoms prior to sampling. Despite these limitations, we still found that an acute viral infection can exert a small but significant shift in the bacterial flora, supporting our previous findings in the LAIV (EX) cohort. Further taxonomic assessments were not pursued in the FL given the degree of heterogeneity in this group.

Within a cohort, microbiome variability may be attributed in a small part to sampling and sequencing variability, but more largely, to differences between individuals. Environmental conditions of a body habitat have been seen to limit microbiome variability; thus a comparison of the microbiome's variability between cohorts may provide information about changing conditions of a body habitat due to treatment. This variability can be measured by first quantifying the microbiome variance within each cohort, and then testing for heteroscedasticity (i.e., non-constant variance) across cohorts. An analysis comparing the level of within group variability over time was performed based on the Bray-Curtis dissimilarities within each group (EX, FL or HV by visit), as measured by the average distance of samples from the centroid of each group. This analysis revealed a reduction in variability among the LAIV treated subjects

at visits 2 and 3, compared to visit 1 (p < 0.0001 for both) **(Figure S1).** FL and HV

variance remained constant, i.e. was not heteroscedastic. This decrease in microbiome

variability within the LAIV cohort further supports the notion that the LAIV treatment had

an effect on the nasal habitat of the EX cohort. This may imply that conditions of the

nasal habitat were changed by LAIV inoculation such that less variability in the

microbiome was supportable.

LAIV led to an increase in relative abundance of Firmicutes phylum and

Staphylococcus genus.

We next examined how the nasal microbiome changed at the genus and phylum levels

following LAIV versus saline administration. Analysis of the sequences for the V3-V5

regions revealed the presence of 4 prominent phyla (*Actinobacteria*, *Firmicutes*,

Proteobacteria and *Bacteroidetes*), which accounted for more than 90% of all

discovered taxa (**Table 3**). Over 75% of the sequences mapped to 12 genera, 7 of

which were ubiquitous in more than 95% of the samples (*Corynebacterium*,

Propionibacterium, *Staphylococcus*, *Streptococcus*, "Bacilli Class" and *Bacillales*). At

baseline, the relative abundances of most of the major genera in either the EX or HV

groups were comparable in terms of the order, although the mean values differed,

demonstrating inter-subject variability. *Corynebacterium* had the highest mean

abundance, followed by *Staphylococcus*. The relative abundance of the major genera

within individuals was similar between V1-V3 and V3-V5 regions. The only exception

was *Moraxella*, which was unexpectedly detected in high abundance in samples from 2

individuals in the HV group by V3-V5 sequencing, but not by V1-V3.

8

Since we expected our interventions would have the highest effect at the first follow-up visit, we compared first visit and second visit samples on a taxon-by-taxon level utilizing a Ubiquity-Ubiquity (U-U) plot. The U-U plot visualizes how the ubiquity, i.e. the prevalence, of a taxon differs between two groups at matching abundance levels, which provides a means for identifying individual taxa candidates that are the most modulated between two groups, even at low abundance. The U-U plot comparing the first and second visits of the EX and the HV cohort with detectable levels (set to a threshold of 0.5% relative abundance) of individual genera can be found in (**Figures 4, S2**). We found that a higher percentage of subjects had *Bacteroides* and *Staphylococcus* present at visit 2 following LAIV administration. Interestingly, *Bacteroides* was undetectable in all subjects in the EX and HV groups at baseline, but reached a relative abundance of 10% or more in 4/10 subjects in the EX group at visit 2. In addition, we identified the core taxa in each group by examining individual Ubiquity-Abundance (Ub-Ab) distributions of each group of samples (**Figure S3**). At a ubiquity threshold of 80% and relative abundance threshold of 0.5%, *Corynebacterium*, *Staphylococcus* and *Propionibacterium* emerge as the core taxa at both time points in the HV group and at the first visit in the EX group. The core taxa expanded by the second visit in the EX group to include *Staphylococcus*, *Streptococcus*, *Corynebacterium*, *Propionibacterium*, and *Bacillales*. Hence, although the nasal microbiome on the whole appears to be fairly stable over time, we did observe greater changes in individual taxa in the group receiving LAIV compared to the saline nasal spray recipients.

We next examined changes in the relative abundances of individual bacterial taxa, focusing on the most abundant bacterial taxa after LAIV administration (**Figure 5**). We observe from the V3-V5 data absolute changes in the relative abundances of the most changed OTUs over time. While the HV group displayed little change from baseline, the LAIV group had a notable decrease in the relative abundance of *Corynebacterium* and statistically significant increases in *Staphylococcus* and *Bacteroides* ($p < 0.05$ for both by Wilcoxon rank sum testing). Alternatively, such findings may also be explained by a reduction in other taxa and therefore may not represent an explicit increase in burden, but could imply a greater relative representation.

Given that *Staphylococcus* species could cause invasive infections, we examined the temporal changes of this genus. At baseline, 4 out of the 7 subjects in the HV group and 5 out of 10 subjects in the LAIV group had *Staphylococcus* detectable at a relative abundance above 10%. Over time, the relative abundance of *Staphylococcus* in these individuals remained high (>10%). Among the individuals who began with a relatively lower baseline level of *Staphylococcus* (i.e., below 10%), the 3 subjects in HV group continually demonstrated low levels of *Staphylococcus* throughout the study. In contrast, all of the 5 subjects in the EX group who began with a relative abundance of *Staphylococcus* below 10% demonstrated a relative increase in abundance after LAIV administration, which subsequently remained elevated during the study (range 7-33% at visit 2, 13-46% at visit 3; **Figure S4**). Hence, it appears that there are likely intrinsic factors that govern *Staphylococcus* persistence in the nares at a relatively high level in certain individuals over time. However, in a subset of individuals who do not have relatively high baseline levels of *Staphylococcus*, LAIV administration may be

10

associated with increased colonization and persistence of *Staphylococcus* species, although the precision of our sequencing could not identify which individual species were present.

Correlations between different genera

To ascertain if there was any correlated relative abundance amongst the bacterial genera identified, we performed a correlation analysis. Given the compositional aspect of the relative abundance data, the data were transformed to eliminate its inherent bias. To accomplish this, we subjected the data to an additive log ratio transformation by dividing each of the 30 most abundant genera by the sum of the relative abundances of the non-top 30 genera, followed by natural log transformation (29). A correlation matrix was constructed for the most abundant genera, (**Table S1**) revealing consistently positive correlations between *Corynebacterium*, *Staphylococcus*, and *Propionibacterium* (p <0.05 after correcting for multiple testing by false discovery rate), suggesting that the most abundant genera move in unison. The finding that the *relative* abundance of *Corynebacterium* decreased in relation to other measured taxa - while at the same time was shown to be positively correlated with them when transformed to disrupt the compositional nature of the data - can be reconciled by the likelihood that *Staphylococcus* may in fact be expanding at a more rapid pace than *Corynebacterium*.

LAIV induces changes in nasal epithelial gene expression profiles, promoting the
expression of interferon type I & II stimulated genes

To determine whether bacterial colonization might be influenced by host immune
responses to LAIV, we concurrently sampled the nasal epithelium at each visit to
examine host gene expression by microarray analysis. A total of eighteen samples were
obtained from 6 subjects in the EX group and 3 subjects in the HV group concurrently
with microbiome sampling (i.e., baseline and 7-10 days after LAIV or saline spray).
Selecting for differentially expressed genes over time with absolute $\log_2$ fold change
greater than 0.7 and p-value less than 0.01 revealed 297 differentially expressed genes
in the HV group and 58 differentially expressed genes in the EX group. Hypergeometric
testing for the enrichment of GO terms in the up-regulated gene expression list for the
EX group revealed 22 meaningful biological process, all related to immune responses
and most related to antigen processing or lymphocyte activation (**Fig 6, Table S2**). The
enriched GO terms in the HV group, however, revealed only 8 biological processes that
were non-specific, many of which involved ciliary function (**Table S3**). Gene set
enrichment testing, which was corrected for inter-gene correlation, showed a statistically
significant up-regulation in both type I (**Figure 7A**) and type II (**Figure 7B**) interferon-
stimulated genes in the EX group when compared to expression in HV group

Effect of type I IFN on persistence of Staphylococcus aureus in murine nasal
model of colonization.

      Given the robust induction of IFN signature genes following live attenuated
influenza vaccine in the host transcriptional response, we sought to determine whether

IFNs could enhance nasal colonization of *S. aureus*. We first established a mouse model of *S. aureus* nasal colonization (based upon work by Kiser, et al (30)), but specifically used a methicillin resistant strain of *S. aureus* given the epidemiologic importance of secondary MRSA infections following influenza. We found that WT mice develop more persistent *S. aureus* levels following intranasal instillation of MRSA compared to animals deficient in the type I IFN receptor (IFNAR KO) or type II IFN receptor (IFNGR KO, **Figure 8A**). To mimic the effects of LAIV on the interferon response, we next pretreated animals with intranasal poly I:C, which is a synthetic compound that mimics dsRNA present during viral infections, including influenza. We have previously shown that similar to influenza, poly I:C induces type I IFN and type II IFN production, as well as downstream IFN-inducible genes such as IP-10 (31). We examined whether MRSA persistence was dependent upon type I IFN, type II IFN, or both by administering intranasal poly I:C for 3 days to WT, IFNAR KO and IFNGR KO animals, followed by intranasal MRSA instillation. We found that type I IFNs appear to promote the persistence of MRSA in the nares, as the animals deficient in type I IFN receptor had decreased bacterial burden (**Figure 8B**). This suggests that type I interferons may contribute to the persistence of nasal *Staphylococcus* species, including MRSA.

DISCUSSION:

Upper respiratory viral infections are frequently complicated by secondary bacterial infection. Accordingly, we sought to determine whether an influenza virus infection might lead to changes in the nasal microflora, thereby providing insights into

interactions between host response and bacterial community structure. Previous studies include cross-sectional surveys of various upper respiratory samples from patients with pandemic H1N1 influenza infection (32, 33) and oropharyngeal samples from inpatients with acute viral infections (34). These studies revealed no clear "post-viral signature microbiome" given the considerable heterogeneity in bacterial composition among individuals. In contrast, we obtained serial samples during viral perturbation to detect within subject changes in order to provide greater statistical power for our analyses. Additionally, our study is the first to compare dynamic changes of the nasal microbiome and host gene expression from baseline after an acute influenza challenge when compared to saline receiving controls. This design permitted us to contrast the magnitude of effect by a targeted viral stimulus against stochastic time-dependent differences. Despite our limited sample sizes, our approach allowed us to demonstrate small but significant differences in bacterial community structure and host immune response after viral perturbation.

As anticipated, we observed great intersubject heterogeneity of the nasal microbiome. Only upon accounting for intersubject heterogeneity were we able to demonstrate significant, albeit small, changes in community structure with viral perturbation, based on Bray-Curtis similarities. These differences were more evident after LAIV administration and 1-2 weeks after presentation with flu-like illness. In concert, we detected small but significant increases in (within sample) diversity of the microbiome after LAIV administration, without change in these indices in the control group over time. These small effects may be attributed to small sample sizes in general, greater heterogeneity in the flu-like illness group with regards to severity, type and

duration of illness, and inherently limited perturbation in the group with LAIV administration. In this regard, our study underscores the value of repeated measures in microbiome studies.

Similar to earlier studies, we observed a general preponderance of 3 dominant phyla, Actinobacteria, Firmicutes, and Proteobacteria, in all nasal samples (35). Core membership in the HV group over time and the EX group prior to perturbation consisted of only 3 core genera- *Staphylococcus*, *Corynebacterium* and *Propionibacterium*. The core membership expanded after LAIV administration to include *Streptococcus* and *Bacillales,* among others.

Notably, the number of subjects and our sequencing depth were greater than an earlier study examining the nasal microbiome pre- and post-rhinovirus experimental challenge (35), which enhanced our ability to detect significant differences in individual bacterial taxa. We were able to detect a significant increase in *Staphylococcus* relative abundance after LAIV administration. The difference in *Staphylococcus* abundance between the groups receiving saline or LAIV was particularly striking among subjects with low baseline levels of *Staphylococcus*. Although we were unable to confidently assign species of *Staphylococcus,* our animal data demonstrated that induction of an antiviral immune response promotes persistence of *S. aureus*. This supports a recent study where LAIV administration enhanced nasal colonization by MRSA and *S. pneumoniae* in a murine model (36). Future studies will delve into the mechanisms by which *Staphylococcus* species may be permitted to outgrow other commensal bacteria in the upper respiratory tract. Interestingly, we also observed the emergence of *Bacteroides*, an obligate anaerobe, after intervention in the EX group. While the

absolute change was statistically significant in that group, the relative abundances were low, and the clinical relevance of this finding is not clear.

Intertaxonomic bacterial interactions are of interest in determining how the microbiome is shaped within individuals. Of mounting interest in the study of the nasal microbiome is the determination of factors associated with the carriage of potentially pathogenic bacteria, including *S. pneumoniae* and *S. aureus*. Either of these organisms, when implicated in co-infection, leads to poorer clinical outcomes during influenza infection (2, 6, 17, 37, 38). This link has prompted numerous investigators to seek associations or interactions between these pathogenic organisms and what may be considered "normal" commensals. Many studies have reported an observation similar to ours, where the relative abundance of *Staphylococcus* is inversely proportional to the relative abundance of *Corynebacteria* (39). In support of this finding, Yan et al demonstrated the inhibition of *S. aureus* by *C. pseudodiptheriticum* in vitro (40). In parallel, Frank et al (41) found that hospitalized patients had Firmicutes dominant profiles (relative abundance of 71%) while the relative abundance of Actinobacteria proved smaller (20%), supporting a pre-pathogenic potential in compromised hosts. This seemingly exclusive competition was also shown in a study by Uehara et al (42) where a previously harvested strain of *Corynebacterium* was implanted in the nares of *S. aureus* carriers, leading to an eradication rate of 71%, a result not replicated by saline or *S. epidermidis* implantation. However, given that microbiome data is compositional in nature, taxonomic correlations require transformation (e.g., alr transformation) to avoid spurious correlations caused by scaling. Hence, our conclusions differ in that the 3 most abundant taxa (*Staphylococcus*, *Corynebacterium*,

and *Propionibacterium*) appear to be positively correlated, which we believe reflects an overall stability in the bacterial community. These findings suggest that the factors that govern overall microbiome composition are in fact remarkably complex. Rather than focusing on individual bacterial proportions per se, perhaps a better grasp of the ecological characteristics of the nasal niche obtained via host and microbial metagenomic analysis might provide mechanistic insights into why certain bacteria persist in different individuals.

Since host immune response is one potential factor governing the changes in the bacterial composition, we obtained concurrent host response gene expression data pre- and post-LAIV administration. Despite their essential role in antiviral immunity, studies from our group and others have shown that the type I and II interferon responses are associated with suppression of the anti-bacterial component of the innate immune system in animal models of influenza and bacterial co-infections. (19, 20) (23). Moreover, type I IFNs are associated with enhanced colonization by *S. pneumoniae* in a murine model of nasal bacterial colonization (18). Hence, we designed our study to determine whether experimental intranasal administration of LAIV (43), which should induce a secretory and systemic immune response that closely resembles the immune response observed after natural infection (26), would induce a IFN-mediated immune signature (44-46). Hypergeometric gene set enrichment by conservative measures showed a statistically significant up-regulation in interferon type I and II stimulated genes in the EX group. Our results support a prominent local immune reaction in the nares after LAIV administration, as well as highlight a substantial role for ISGs after the first week. Hence, we were able to confirm that our experimental intervention did lead to

induction of an interferon immune signature at the time we saw the most significant changes in the nasal microflora following LAIV. Furthermore, nasal administration of a viral ligand in a murine model led to increased persistence of MRSA in a type I interferon dependent fashion. Since, to our knowledge, LAIV has not been reported to predispose to secondary bacterial infection, it is likely that additional immune defects or perhaps structural changes in the respiratory epithelium induced by viral infection are necessary for the development of invasive disease. Nonetheless, increased colonization by potentially pathogenic bacteria may represent a critical first step.

Our study is not without limitations. The number of volunteers in each group was small; however there were 3 samples obtained from each volunteer at different time points, allowing greater power with the benefit of paired statistical methods. Another limitation to our approach was an inability to make confident assignments of species to *Staphylococcus* OTUs due to the less than 3% difference in the V1-V3 regions between *S. aureus* and *S. epidermidis.* Finally, another limitation pertains to culture independent 16S rRNA sequencing and that is the inability to distinguish live organisms from transient microorganism colonization, particularly with the potentially significant quantity of inhaled bacterial burden (47). Additional repeated measures, i.e. increasing sample periodicity, from the same donor across all three treatment cohorts, would improve our understanding of the rate of microbiome change, and its potential variability and limits. This would provide a clearer relationship between donor treatment and cessation of symptoms versus the microbiome's recovery towards "normality". Identifying such lags might provide an avenue for better understanding cause and effect, instead of correlation alone.

In summary, LAIV administration was associated with clinically meaningful changes in nasal epithelial gene expression that mirrored those expected of natural influenza infection, including activation of interferon-stimulated pathways, which have recently been implicated in diminished anti-bacterial activity and enhanced bacterial colonization in murine models. Along with these host gene expression changes, LAIV led to significant changes in bacterial community structure along with increases in the relative abundance of *Staphylococcus*. The nasal microbiome changes after flu-like illness were subtler, presumably due to the heterogeneity in that group. These changes support murine models and clinical findings, suggesting that they represent the first steps towards the emergence of potentially pathogenic bacteria during natural upper respiratory tract infection. Further investigation is needed to better appreciate these complex host-microbiome interactions in true disease states.

MATERIAL AND METHODS:

Enrollment

This study alternately assigned non-blinded cohorts of paid healthy adult volunteers to either LAIV or saline nasal spray (**Figure S1**). Volunteers were between the ages of 18 to 65 years and were without known medical problems. Any subjects with nasal ailments, on immunosuppressive medication (including nasal steroid spray or prednisone dose $\geq$ 20 mg or equivalent), exhibiting respiratory infection or antibiotic use within the last 60 days, or with known chronic conditions were excluded. Upon volunteering, subjects were screened with a questionnaire that obtained general identifiers, contact information and demographics such as age, sex and ethnicity.

Relevant data to the study included prior medical history, medication or probiotic usage. Also addressed were the presence of habitual nose picking and personal hygiene measures including frequency of bathing or showering, as well as swimming. The study was reviewed and approved beforehand by our human subjects institutional review board (UCLA IRB IRB#11-000326).

Sampling

Specimens were collected using sterile, dry swabs (EpiCentre). A total of 4 swabs (2 from left nares, 2 from right) were obtained from each subject at enrollment, and repeated at 1-2 weeks and then 4-6 weeks after initial presentation. In addition, subjects underwent nasal lavage with 10 ml of sterile non-microbiostatic saline at each timepoint. The nasal swabs and lavage from each individual were pooled for isolation of bacterial DNA using the PowerSoil DNA Isolation Kit (Mo-Bio laboratories). V1-V3 and V3-V5 hypervariable regions of the 16S rDNA gene were amplified by PCR with barcoded primers designed using a set of algorithms developed at the J. Craig Venter Institute (JCVI) (48). Amplicons were completed as follows (per reaction): 2 μL of first round amplification product, 0.75 units of Q5® High Fidelity DNA Polymerase (New England Biolabs, MA) and 1× final concentration of Q5® High-Fidelity Master Mix. Primers were added to a final concentration of 200 nM, with dNTPs at a final concentration of 200 μM, along with the Q5 High GC Enhancer for amplification to a 1× final concentration and nuclease-free water to bring the final volume to 20 μL. PCR cycling conditions were: initial denaturation of 30 seconds at 98°C followed by 30 cycles of 98°C for 10 seconds, 30 seconds at 56°C, and 72°C for 60 seconds, followed by a

final incubation at 72°C for 5 minutes before cooling to 4°C. Negative controls were included, which were examined after 35 cycles. PCR reactions were visualized on 1% agarose gels. Each reaction was cleaned individually using the Agencourt XP beads (Beckman Coulter, Inc., Indianapolis, IN) and resuspended in 30 µL of water prior to normalization and pooling of samples for sequencing. Amplicons were quantitated using the Quant-iT PicoGreen dsDNA Assay Kit (Life Technologies, Grand Island, NY) and then normalized amounts of each sample were combined into one pool prior to purification using a QIAQuick PCR Purification column (Qiagen, Valencia, CA), and submitted for sequencing with the Roche-454 FLX Titanium platform. The pooled samples were further cleaned using the Agencourt AMPure system (Beckman Coulter Genomics, Danvers, MA) prior to emulsification PCR (emPCR). Steps for emPCR, enrichment and 454 sequencing were performed by following the vendor's standard operating procedures. Real-time PCR was used to accurately estimate the number of molecules needed for emPCR. Total RNA was extracted from a subset of the specimens and 18 samples were submitted for expression profile analysis by Affymetrix chip hybridization, following manufacturer recommendations.

Microbiome Analysis

After sequencing, a read processing pipeline consisting of a set of modular scripts designed at the JCVI along with the mothur pipeline (49) were employed for deconvolution, trimming and quality filtering. Reads were first deconvoluted or assigned to samples based on their unique 10 nt barcode allowing no more than a one nucleotide mismatch to the barcode. After deconvolution, barcode and 16S primer sequences were

removed allowing a maximum of 6 mismatches to the 16S primer and a maximum

primer to barcode distance of 3 nt. Quality trimming of reads was performed using

mothur. Reads with an average length of <100 nt, and reads with 'Ns' or with

ambiguous base calls or a homopolymer longer than 8 nt were removed from

subsequent analyses. A Blastn quality check was performed against an internal data set

of 16S rRNA gene sequence reads to remove any sample reads not consistent with 16S

rRNA gene sequences, in which at least 30% of the query must be covered by the

alignment (60 nt minimum). Passing reads were subsequently further processed

including chimera checking through the mothur pipeline. After quality control processing,

an average of 8,579 quality reads per sampled remained for further data analysis.

Distance Based Analyses.

Metric multidimensional scaling plots were generated with the help of the Vegan

package in R, with distances based on Bray-Curtis dissimilarities. Inter-sample

comparison with permutational multivariate analysis of variance (PERMANOVA) based

on Bray-Curtis dissimilarities were performed using the Adonis function within the

Vegan package. To control for intersubject variability, the linear model utilized was

distance = Visit + Treatment + Visit x Treatment + error, with stratification by Subject.

The factors under consideration were based on the treatment by visit interaction when

more than two groups were analyzed, versus visit alone when a single group was

analyzed. Results were reported based on bootstrapped p-value and associated

unadjusted R^2. The dispersion analysis was performed by estimating the residuals for

each sample by element-wise multiplying the estimated coefficients matrix ($B_{(p \times n)}$) by

the transposed model matrix $(X_{(n \times p)})'$, where p is the number of regression coefficients estimated and n is the number of samples. With the resultant matrix, the absolute value of each column is summed, thus representing the total residuals associated with each sample. For each possible pair of groups the residual values underlying each group were compared for equality using the non-parametric Wilcoxon rank-sum testing. P-values were not corrected for multiple testing.

Taxonomic Abundance Analyses.

Normalized taxonomic abundance profiles were computed for each taxonomic category by dividing the number of reads assigned to a taxon by the total read count in each sample. The Shannon diversity index was calculated using Vegan, and the tail statistic, which is a rank-based diversity metric for analyzing low abundance taxa, was calculated as described by Li et al [46]. Two-way, repeated measures ANOVA for the tail statistic and Shannon index were individually achieved in JMP version 11. The factors analyzed were visit (as a repeated measure) and study intervention.

For the correlation analysis between taxa, the additive log transform (ALR) was performed by dividing each of the 30 most abundant genera by the sum of the relative abundances of the remaining non-top 30 genera. These ratios were then natural log transformed. To prevent performing the natural logarithm transformation on an abundance of 0, taxa with zero abundance were replaced with 1/10th of the lowest non-zero abundance across all samples and taxa. ALR transformed abundances are less prone to spurious correlation due to normalization since each transformed value is a

ratio between its abundance and the reference "remaining" abundance. The top 30 taxa represented close to 94% of the taxa by abundance.

Corbata Plots.

Core microbiome analysis U-U Plots were generated using Corbata (50). Briefly, for each taxon in a group of samples, the relationship between abundance and ubiquity is calculated. Then for each pair of groups, at matching abundances, a curve is generated to indicate the relative ubiquity of each taxon in each group. See the Material and Methods in Li 2013 (51) for a mathematically rigorous description of the algorithm. For interpretation, if group A and B are represented on the X and Y axis respectively, if a taxon tends to be in greater ubiquity in group A then its curve will meander towards the bottom right of the plot (i.e., deviate from the diagonal line towards the x-axis). If the taxa tends to be in greater ubiquity in group B, then it will meander towards the top left of the plot, or y-axis. When there is no difference between the ubiquity of a taxon between two groups, the curve will trace over with the diagonal reference line. The Ub-Ab plot, also found in the Corbata suite of tools, represents the ubiquity of a taxon across all members of a cohort, as a function of abundance. Core taxa, which tend to be high in abundance and ubiquity can be identified by curves seeking the top right of the plot.

When the sample sizes were relatively small, U-U and Ub-Ab plot curves will be more jagged and step-shaped. Thus, smoothing was performed with bootstrapping by sampling with replacement of both the samples and reads during each bootstrap iteration. Also, frequently the U-U curve between two groups will fall along the diagonal,

signifying that there is not a significant difference between the ubiquity of a taxon at all abundances between two cohorts. To improve visualization, only taxa that were statistically significantly different using the Kolmogrov-Sminorv test are plotted.

Microarray Analysis

For quality control assessment, the Affymetrix chips were inspected visually and felt to be free of gross spatial defects. More detailed analyses of the scanned data were obtained through the affyQCreport package of the Bioconductor project in R (52). Intensity plots of individual chips were comparable, overlapping without outliers. Normalized unscaled standard error (NUSE) plots aligned across all chips. There was also the notable absence of significant variability between the percentage present and average background values in each chip. RNA degradation plots of each chip converged with similar slopes, suggesting agreement in the degrees of RNA digestion. As recommended by the manufacturer, all chips showed appropriate levels of expression for β-actin, though GADPH expression was just above the recommended level on 3 chips (two in the control group and one from the experimental group). Finally, inspection of the positive and negative border elements revealed positive and negative controls grouping in distinct intensity ranges, as expected.

Expression data was extracted using the affybatch package of the Bioconductor project in R. Background adjustment, normalization and summarization were achieved across both sets independently (EX and HV) using the well-established RMA or "Robust Multichip Average" method (53-55). Non-specific filtering was achieved with the nsFilter function, removing 50% of genes with the lowest variance across all the chips, as well

as gene IDs that did not match to an Entrez ID or matched to more than one Entrez ID. After filtering, the lmFit and eBayes functions were used to perform moderated paired t-testing for each gene across visits 1 and 2.

At this level, gene set enrichment of interferon I and II stimulated genes (ISG) was performed with the QuSAGE package in R (56), comparing our processed gene lists against those from a prior study of A549 cell lines subjected to to α or γ interferon (57).

Genes of interest from either group were then selected based on those with absolute $\log_2$ fold changes greater than 0.7 and individual p-values less than 0.01. Both sets of up-regulated genes were subjected to conditional hypergeometric testing via the GOstats package to shed light on any potentially grouped biological processes (58). Only the resultant processes with reported individual p-values of less than 0.001 were reported. A heat map was generated from the gene list obtained from the EX arm using the heatmap.2 function in the gplots package, clustered by gene expression and with supervised labeling of up-regulated GO:BP functions based on prior hypergeometric testing.

Animal model of nasal colonization.

Age- and sex-matched mice with a C57BL/6 genetic background were used in all experiments. Wildtype C57BL/6 (WT), Type I IFN receptor knockout (IFNAR KO), and type II IFN receptor knockout (IFNGR KO) animals were bred and housed in in-house colonies. For nasal colonization experiments, Los Angeles County (LAC) strain of methicillin-resistant *S. aureus* (MRSA) was used. Bacteria were grown overnight in

Tryptic soy broth in a shaking incubator at 37°C, followed by 4 hour subculture the following morning. An innoculum of 6x10^{7} CFU total was placed in the nares of each animal under light anesthesia, followed by nasal lavage with 200 ml of sterile saline 24 hours later. Poly I:C (50 mg in 50 ml) or sterile saline control was nasally instilled daily for 3 days prior to MRSA innoculation, where applicable. Bacterial colony forming units (CFU) were enumerated by plating nasal lavage samples on TSA agar using 1:5 serial dilutions. All animal experiments were performed in accordance with NIH policies regarding the humane care and use of laboratory animals and were approved by the UCLA Office of Animal Research Oversight (OARO protocol 2005-143). Care was taken to minimize pain and suffering where possible.

List of Abbreviations Used:

1. LAIV: Live attenuated influenza vaccine

2. HV: Healthy volunteer group (controls)

3. EX: Experimental group (receiving live attenuated influenza vaccination)

4. FL: Flu like illness group (observational group).

5. GO:BP: Gene ontology : biologic processes

6. ISG: Interferon stimulated genes

Authors' Contributions:

JCD, BAM, and EG conceived and planned the study. SH, CN were involved in primary study design and data collection. YT, KL, BAM and JCD were responsible for the computational analysis and manuscript preparation. EG assisted with data analysis

and manuscript preparation. MB assisted with computational data analysis. KS and BF carried out experiments. KL and BAM were responsible for statistical analysis. XW and DE assisted with statistical analysis.

Acknowledgments:

Tables

Table 1: Characteristics of the volunteers

	Healthy Volunteer Saline Controls (HV) (n=7)	Healthy Volunteer LAIV (EX) (n=10)
Age, mean (range)	21.3 (18-25) years	23.8 (18-32) years
Gender (% female)	23.5%	29.4%
Student (%)	100%	70%
Nose picking:		
Never	14.3%	20%
Weekly	71.4%	50%
Daily	14.3%	30%

Values noted are means with ranges expressed for the age. In addition to that noted above, all volunteers had no recent smoking history, did not swim, predominantly showered rather than bathed and used no probiotics or antibiotics within 90 days of enrollment.

Table 2: Characteristics of patients presenting with flu-like illness

	Flu-like illness (n=19)
Age, mean (range)	32.6 (19-65) years
Gender (% female)	36.8%
Student (%)	31.6%
Nose picking:	
Never	31.6%
Weekly	36.8%
Daily	31.6%

Values noted are means with ranges expressed for the age. In addition to that noted above, 2 patients currently smoked, while another 2 both showered and bathed. None swam, used no probiotics or antibiotics within 90 days of enrollment.

Table 3: Mean relative abundance of detected phyla and genera by group and visit.

Phylum	Genera (in italics)	HV (Controls)				EX (LAIV)		
		Visit 1	Visit 2	Visit 3		Visit 1	Visit 2	Visit 3
Actinobacteria		37.46%	38.94%	35.42%		45.97%	23.52%	38.96%
	Corynebacterium	24.89%	25.75%	25.16%		34.44%	15.40%	30.86%
	Propionibacterium	10.29%	11.09%	8.00%		6.66%	6.21%	5.35%
	Actinomycetales	1.41%	1.62%	1.60%		3.09%	1.42%	2.16%
Firmicutes		32.18%	25.56%	41.56%		40.71%	51.34%	44.99%
	Staphylococcus	16.14%	12.79%	25.28%		19.04%	26.37%	24.53%
	Streptococcus	1.11%	2.14%	0.49%		8.37%	4.68%	4.26%
	Bacilli Class	2.67%	2.10%	4.10%		3.60%	4.80%	4.32%
	Bacillales	1.87%	1.37%	2.74%		1.85%	2.56%	2.55%
Proteobacteria		23.91%	30.29%	13.34%		5.28%	6.92%	5.01%
	Moraxella	11.66%	22.16%	10.51%		0.68%	0.02%	0.12%
	Pseudomonas	7.59%	3.12%	0.87%		0.03%	1.26%	0.07%
	Enterobacteriaceae	0.92%	1.20%	0.18%		3.29%	1.69%	0.47%
Bacteroidetes		1.40%	0.85%	0.04%		2.60%	7.87%	4.95%

	Bacteroides	0.00%	0.00%	0.01%		0.00%	6.26%	4.13%
Cyanobacteria		1.36%	1.85%	1.41%		1.04%	3.66%	3.65%
	Streptophyta	1.21%	1.79%	1.40%		1.03%	3.58%	0.88%
Fusobacteria		0.042%	0.023%	3.88%		0.61%	1.78%	1.17%
Phylum Cumulative		96.35%	97.51%	95.65%		96.21%	95.09%	98.73%
	Genera Cumulative	79.76%	85.13%	80.34%		82.08%	74.25%	79.70%

The above shown are average relative abundances of the 6 most abundant phyla and 12 most abundant genera by group. Phyla are noted in bold with identified genera beneath. All OTUs had a ubiquity of over 90% except *Moraxella*, *Pseudomonas*, Enterobacteriaceae and *Bacteroides*. *Bacteroides* was notably almost exclusively present in the EX groups on visits 2 and 3. Cumulative genera and phyla representation is noted at the bottom.

Supplemental Tables

Table S1: Significant correlations among the most abundant genera

Staphylococcus	Corynebacterium	Propionibacterium	Moraxella	Dolosigranulum	Streptococcus	Peptoniphilus	Haemophilus	Streptophyta	Anaerococcus	
									-	Anaerococcus
								-	0.37	Streptophyta
							-	-	-	Haemophilus
						-	-	0.26	0.68	Peptoniphilus
					-	-	0.30	-	-	Streptococcus
				-	-	-	-	-	-	Dolosigranulum
			-	-	-	-	-	-	-	Moraxella
		-	-	-	-	0.53	-	0.31	0.60	Propionibacterium
	-	0.55	-	0.52	-	0.41	-	-	0.49	Corynebacterium
-	0.32	0.57	-	-	-	0.43	-	0.34	0.50	Staphylococcus

Table S2: Hypergeometric testing for the enrichment of GO:BP terms in the EX (LAIV) group

	GO:BP ID	P-value	Odds Ratio	Exp Count	Count	Size	Term
1	GO:0006952	5.09E-08	7.89	3.50	16	765	defense response
2	GO:0019884	4.51E-06	17.01	0.45	6	98	antigen processing and presentation of exogenous antigen
3	GO:0002449	7.52E-06	15.47	0.49	6	107	lymphocyte mediated immunity
4	GO:0048002	7.94E-06	15.32	0.49	6	108	antigen processing and presentation of peptide antigen
5	GO:0002526	7.94E-06	22.19	0.28	5	62	acute inflammatory response
6	GO:0002253	8.99E-06	9.54	1.09	8	239	activation of immune response
7	GO:0002682	1.18E-05	5.99	2.88	12	629	regulation of immune system process
8	GO:0002252	1.40E-05	7.76	1.54	9	337	immune effector process
9	GO:0072376	1.54E-05	32.73	0.16	4	34	protein activation cascade
10	GO:0030449	5.70E-05	51.01	0.08	3	17	regulation of complement activation
11	GO:0006958	8.08E-05	44.63	0.09	3	19	complement activation, classical pathway
12	GO:0060333	9.14E-05	19.99	0.24	4	53	interferon-gamma-mediated signaling pathway
13	GO:0016064	0.0001	18.47	0.26	4	57	immunoglobulin mediated immune response
14	GO:0019886	0.0001	17.79	0.27	4	59	antigen processing and presentation of exogenous peptide

							antigen via MHC class II
15	GO:0002504	0.0002	17.16	0.28	4	61	antigen processing and presentation of peptide or polysaccharide antigen via MHC class II
16	GO:0006959	0.0002	16.30	0.29	4	64	humoral immune response
17	GO:0002824	0.0004	24.58	0.15	3	32	positive regulation of adaptive immune response based on somatic recombination of immune receptors built from immunoglobulin superfamily domains
18	GO:0034341	0.0004	13.01	0.36	4	79	response to interferon-gamma
19	GO:0002460	0.0004	13.00	0.36	4	87	adaptive immune response based on somatic recombination of immune receptors built from immunoglobulin superfamily domains
20	GO:0006957	0.0006	76.96	0.04	2	8	complement activation, alternative pathway
21	GO:0050778	0.0006	21.10	0.17	3	47	positive regulation of immune response
22	GO:0071345	0.0009	6.15	1.17	6	255	cellular response to cytokine stimulus

Gene selection thresholds are p value < 0.01 and $\log_2 FC > 0.7$.

Table S3: Hypergeometric testing for the enrichment of GO:BP terms in the HV (control) group

	GO:BP ID	P-value	Odds Ratio	Exp Count	Count	Size	Term
1	GO:0001539	2.766E-06	2.909E+01	2.346E-01	5	22	ciliary or bacterial-type flagellar motility
2	GO:0060271	7.805E-06	9.180E+00	1.034E+00	8	97	cilium morphogenesis
3	GO:0044782	2.029E-05	9.677E+00	8.529E-01	7	80	cilium organization
4	GO:0003341	6.236E-05	2.296E+01	2.239E-01	4	21	cilium movement
5	GO:0035083	6.283E-05	5.786E+01	8.529E-02	3	8	cilium axoneme assembly
6	GO:0007018	1.689E-04	8.295E+00	8.318E-01	6	82	microtubule-based movement
7	GO:0030031	2.163E-04	5.551E+00	1.642E+00	8	154	cell projection assembly
8	GO:0048609	7.051E-04	3.549E+00	3.529E+00	11	331	multicellular organismal reproductive process

Gene selection thresholds are p value < 0.01 and $\log_2$FC > 0.7.
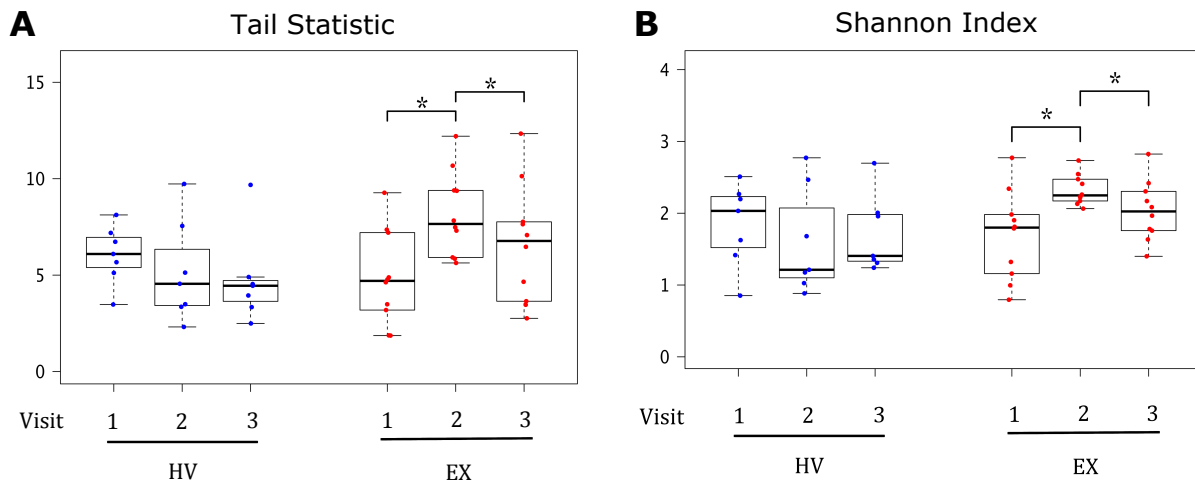
Figures

Figure 1: Measures of diversity in EX and HV groups, by visit. Panels A demonstrates calculated tail statistics at all time points for either group (EX V1 to V2 p = 0.020 ; EX V2 to V3 p = 0.017). Panel B demonstrates Shannon indices for all time points (EX V1 to V2 p = 0.014 ; EX V2 to V3 p = 0.049). (*, p<0.05).
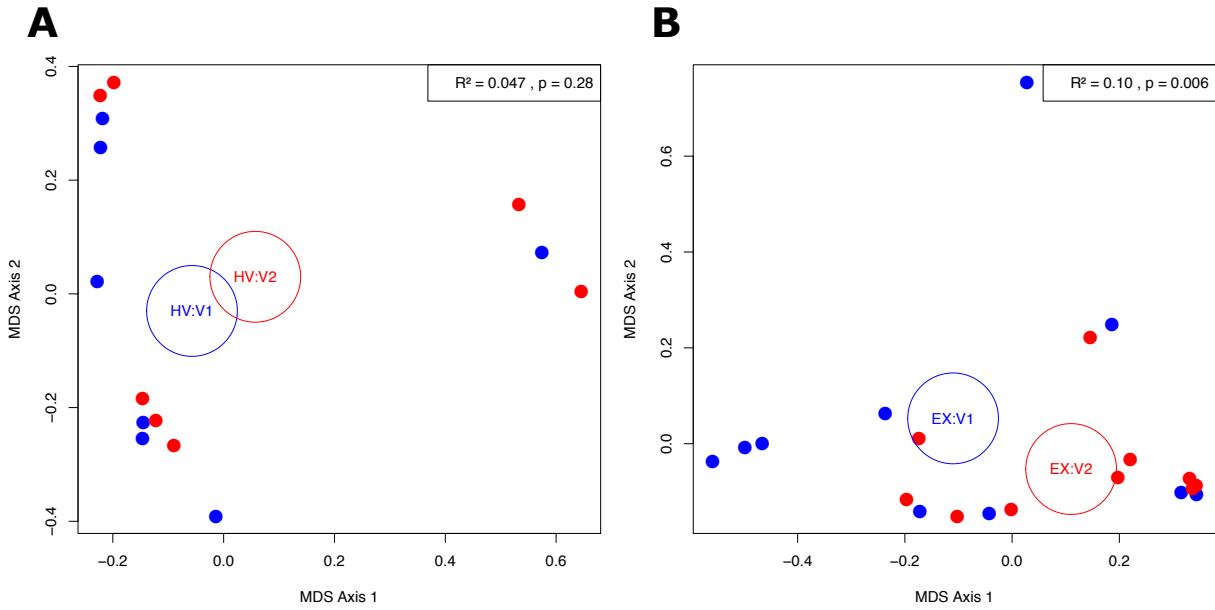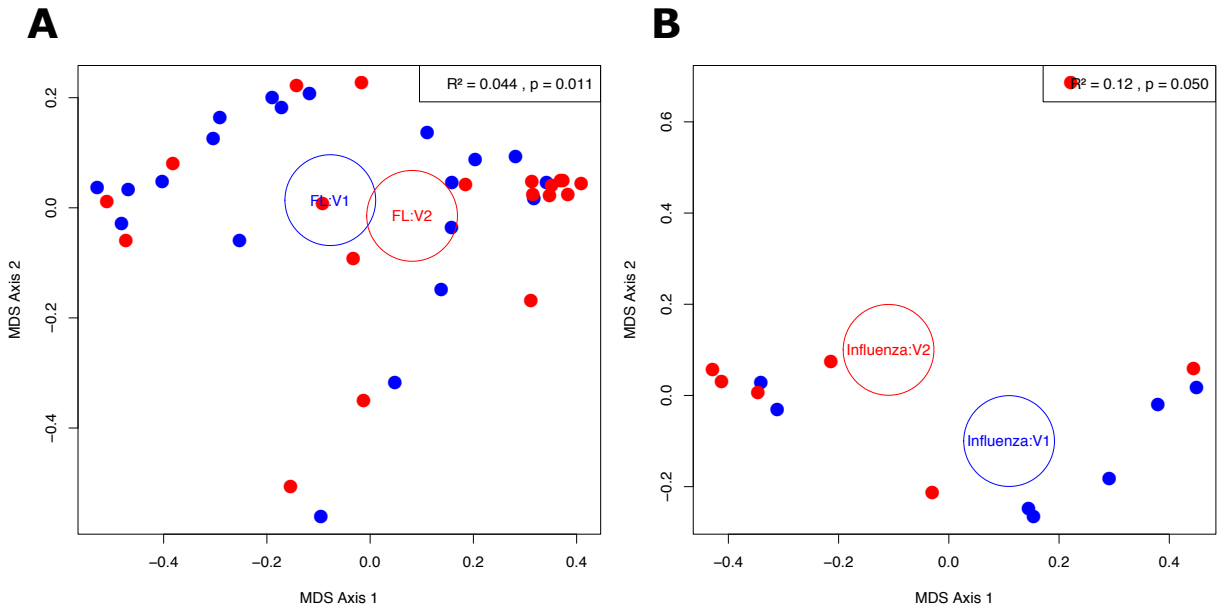
Figure 2: Multidimensional scaling plots demonstrating dissimilarities by Bray-Curtis indices between the first two visits in the HV (Panel A) and EX (Panel B) groups. Data points from the first visits are in blue, while the second visits are in red. Circles represent respective centroid locations.

Figure 3: Multidimensional scaling plots demonstrating dissimilarities by Bray-Curtis indices between the first two visits in the Flu-like (Panel A) and Influenza positive (Panel B) groups. Data points from the first visits are in blue, while the second visits are in red. Circles represent respective centroid locations.
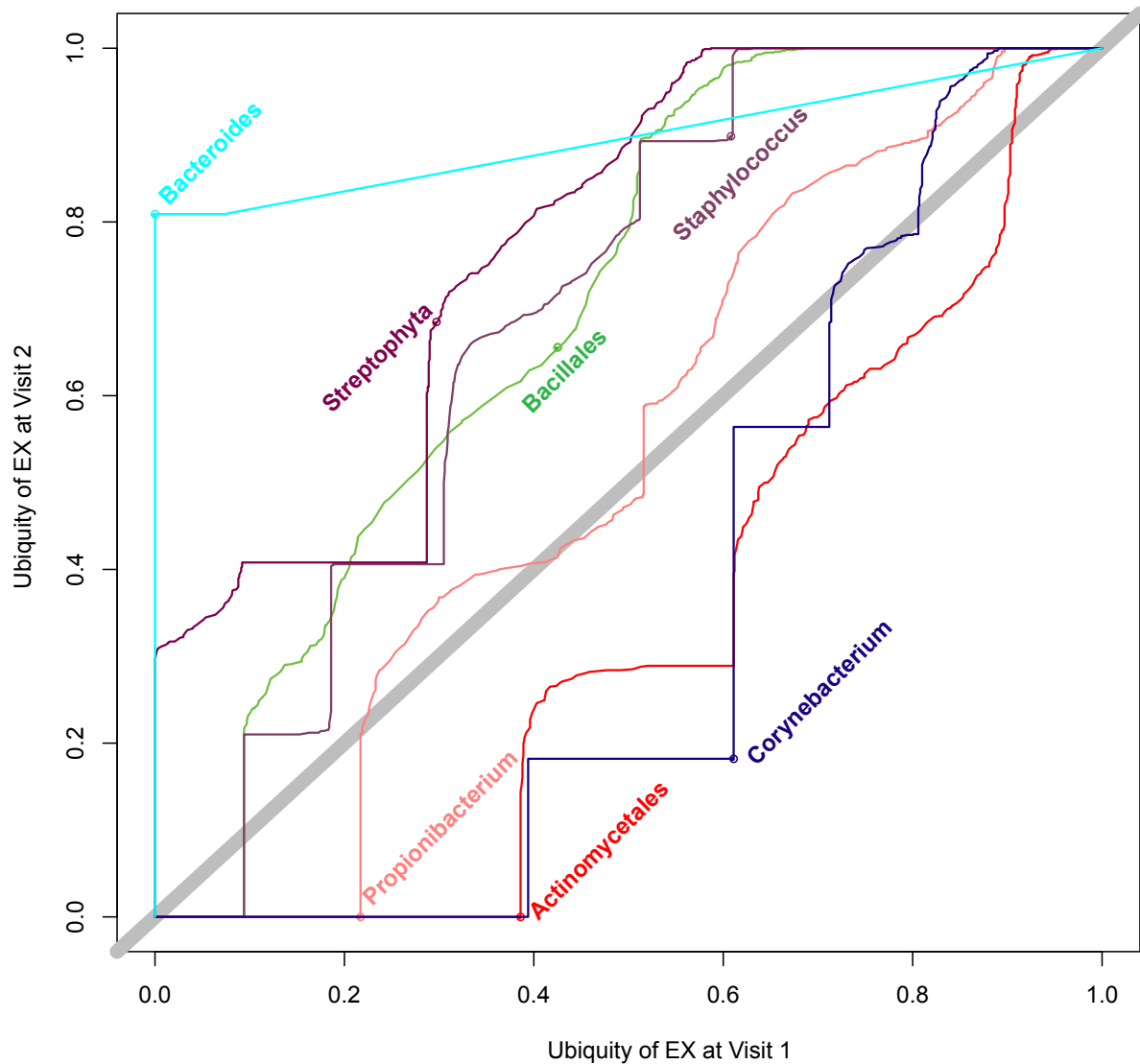
Figure 4: Ubiquity-ubiquity plot depicting the change in ubiquities for selected taxa, across the range of relative abundances between visits 1 and 2 in the EX group. Only OTUs with a relative abundance greater than 0.5% were scored as "present," and only OTUs with a change in ubiquity greater than 20% were included in this plot. OTUs that aligned to the right of the diagonal were more ubiquitous during visit 1, while those to the left were more ubiquitous at visit 2.
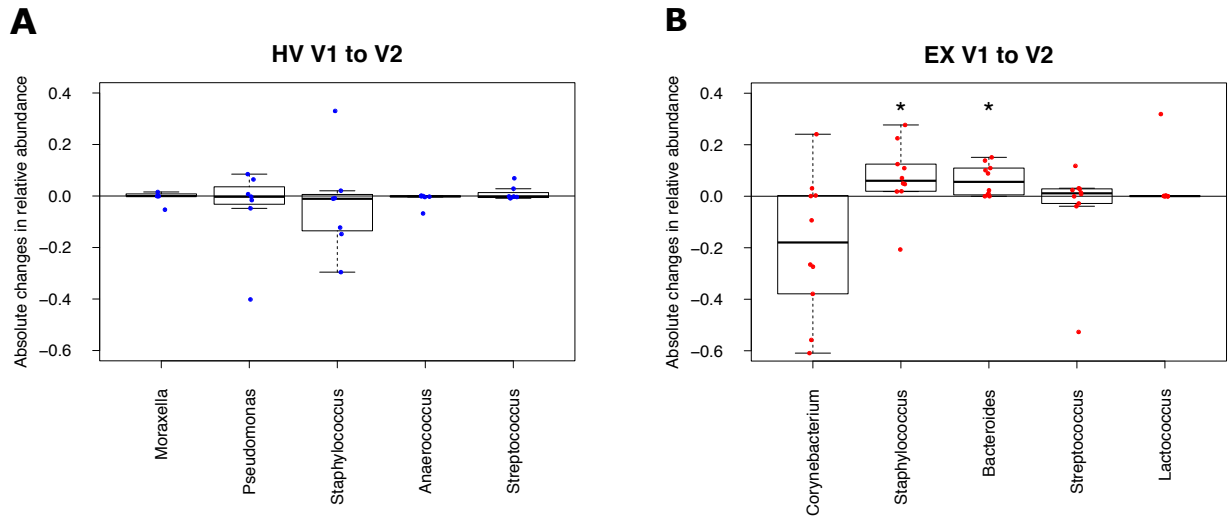
Figure 5: Absolute changes in relative abundance in the top 5 changed taxa in the HV (Panel A) and EX (Panel B) groups (in the EX group, *Staphylococcus* p = 0.048, *Bacteroides* p = 0.013). (*, p<0.05).
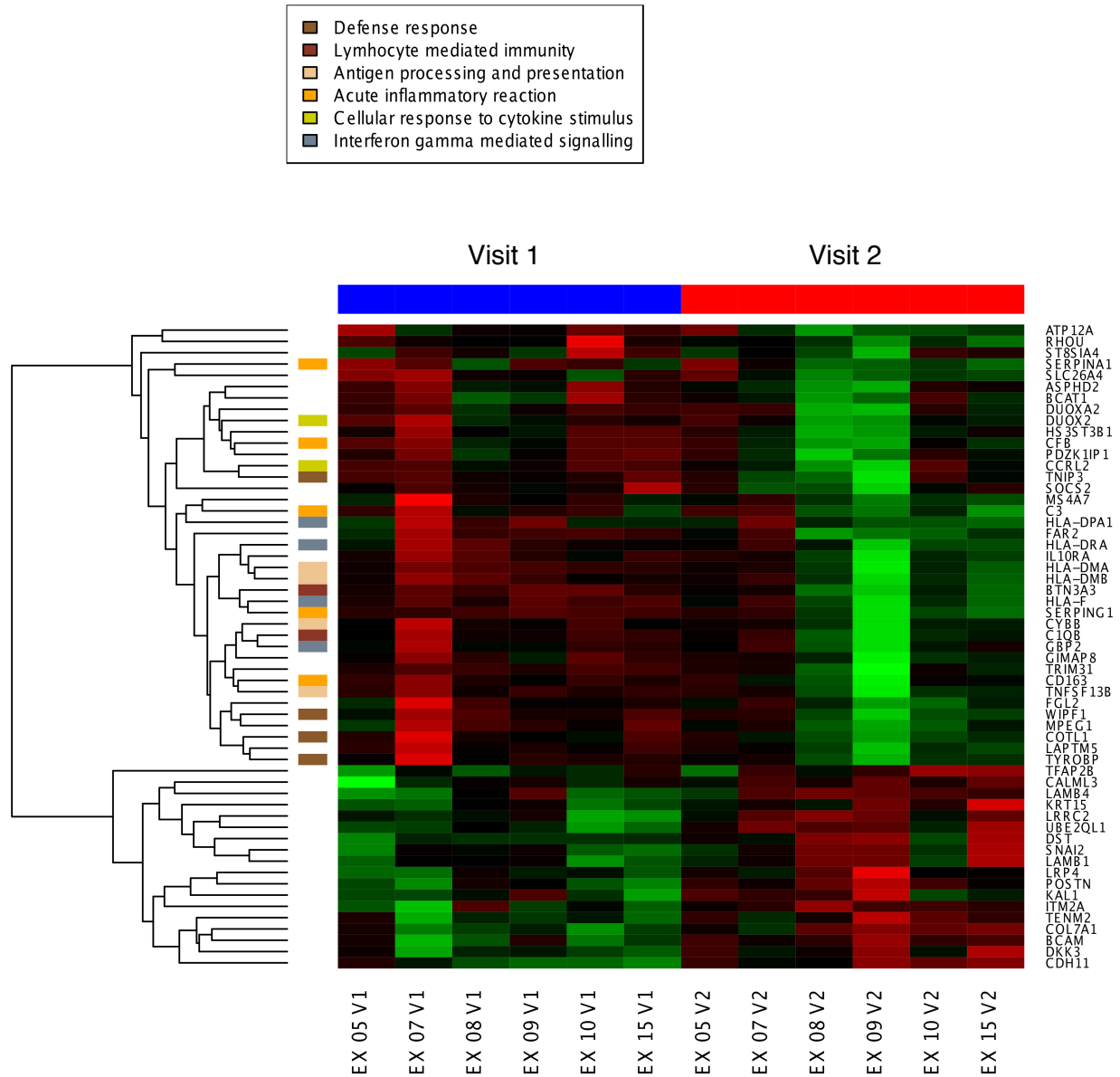
Figure 6 A heat map of log$_2$ gene expression for the most differentially expressed genes in the EX group, selected by thresholds of p-value < 0.01 and log$_2$ fold changes greater than 0.7 between visits. The left hand column shows selected gene ontology associations from the hypergeometric GO:BP analysis as described. Given significant overlap between gene ontology terms, representative groups were chosen to represent as many unique and non-overlapping GO:BP terms as possible.
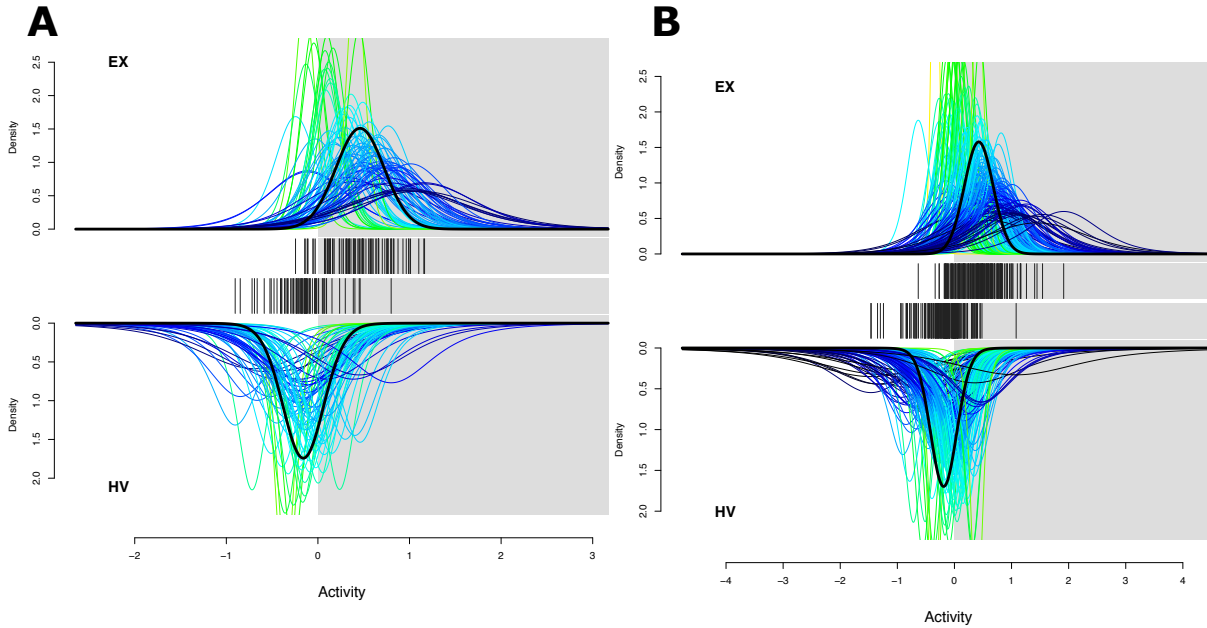
Figure 7: Gene set enrichment analysis for type I (A) and type II (B) interferon-stimulated genes in our expression sets. These figures demonstrate a probability density function for each gene, the center of which is marked by a vertical line on each x-axis. Distributions that lie predominantly to the right of the 0 mark are more likely up-regulated, while those to the left are not. The sum of these functions, corrected for inter-gene correlation, is represented by a thick black distribution for each group. The EX group is shown on the upright graph and the HV group is drawn in the opposite direction for comparison. The EX group showed significant gene set enrichment in both type I and II interferon sets, when compared with the HV group (p<0.05).
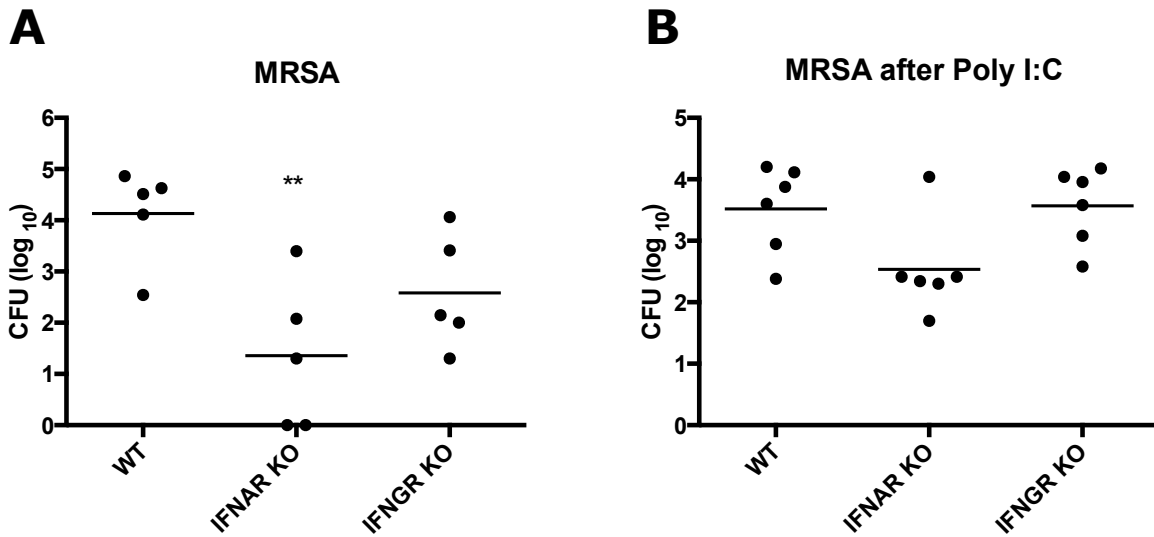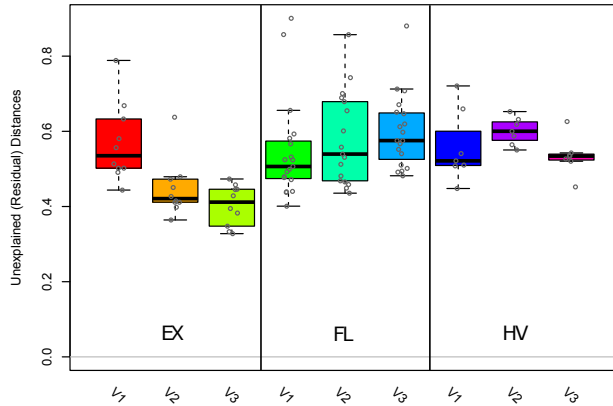
Figure 8: *S. aureus* colonization after poly I:C is type I interferon dependent. Wildtype, IFNAR, and IFNGR knockout mice were administered intranasal poly I:C (50 mcg) daily for 3 days, followed by i.n. MRSA (6.7×10^7 CFU). Twenty-four hours later, nasal lavage was performed for enumeration of CFU. (** = $p<0.01$).
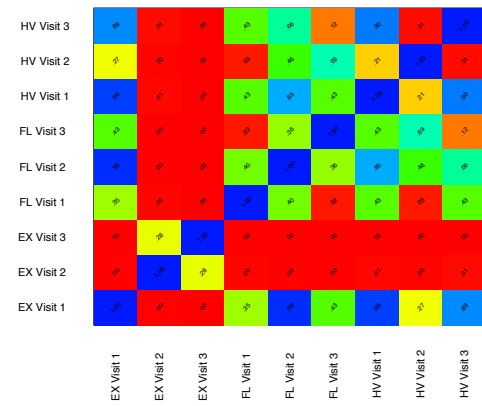
Supplemental Figures

Figure S1: Panel A demonstrates dispersion from the individual centroids for all groups across three visits based on Bray-Curtis dissimilarities in the aforementioned all-inclusive PERMANOVA model. Panel B shows resultant p-values for each comparison between these groups.
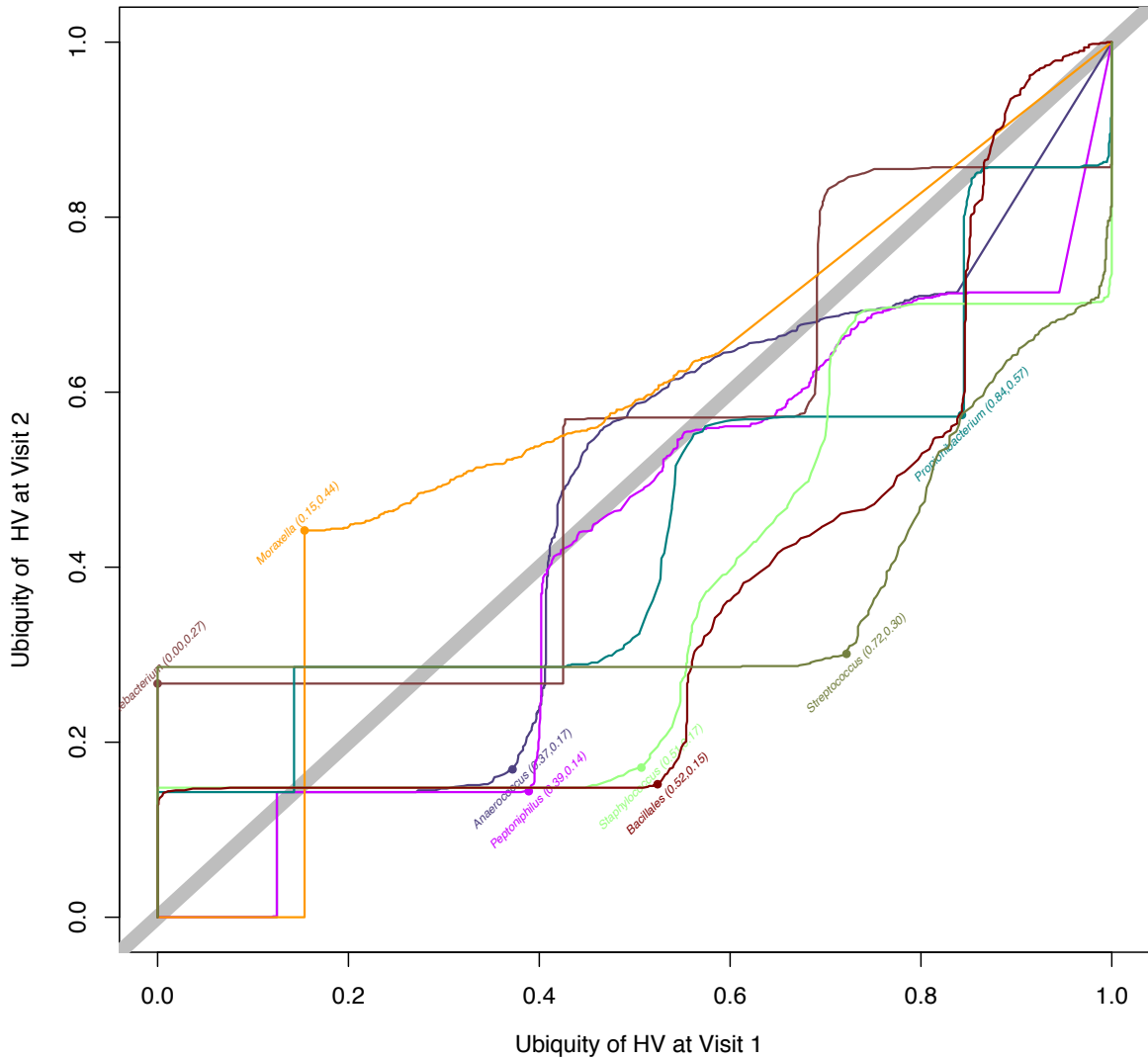
Figure S2: Ubiquity-ubiquity plot contrasting the ubiquities of a number of selected taxa, across a range of relative abundances between visits 1 and 2 in the HV group. Only OTUs with a relative abundance greater than 0.5% and change in ubiquity greater than 20% were included in this plot. OTUs that aligned to the right of the diagonal were more ubiquitous during visit 1, while those to the left were more ubiquitous at visit 2.
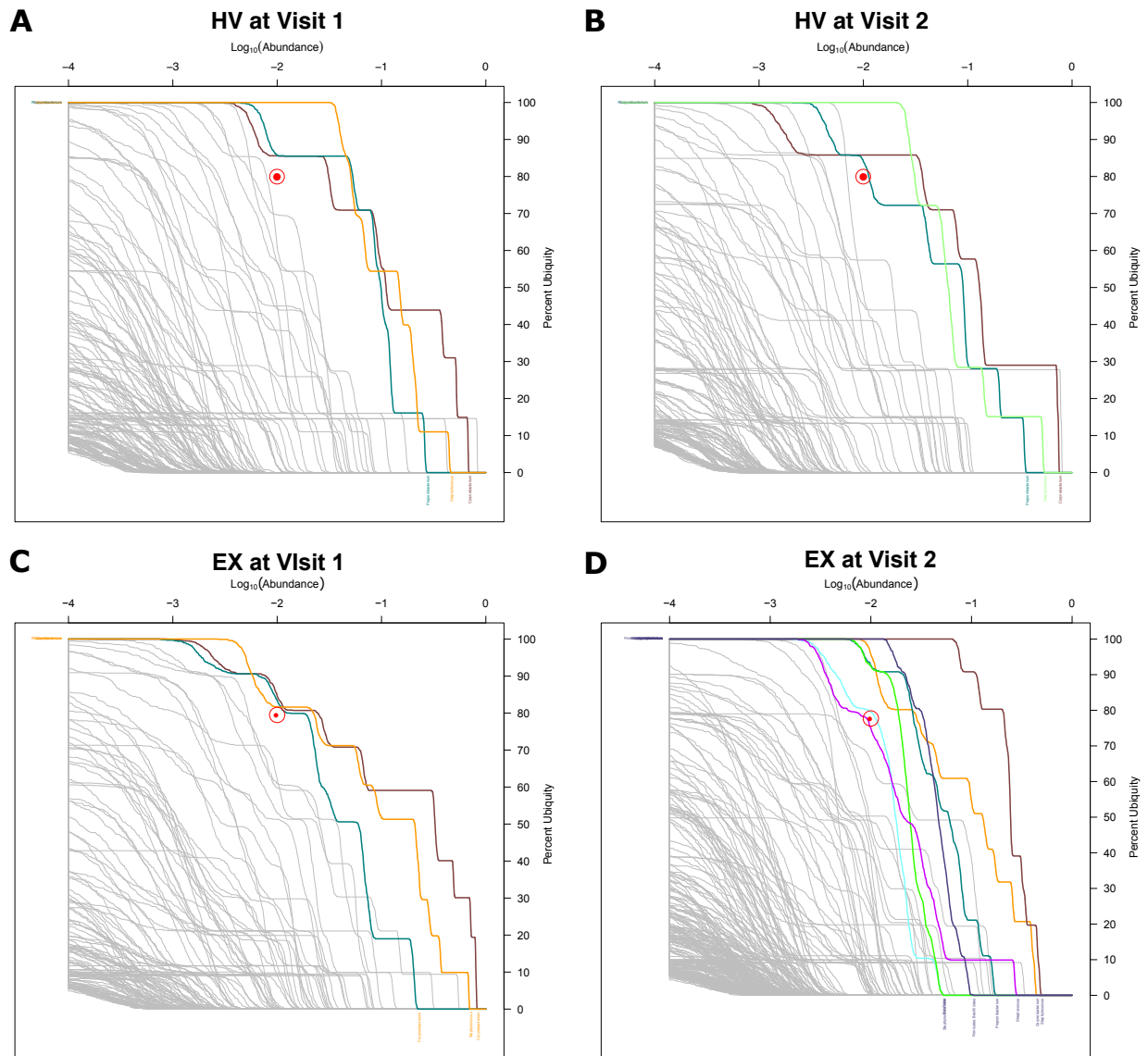
Figure S3: Ubiquity-abundance plots for each group, by visit. These figures plot OTU ubiquities across a range of relative abundances, highlighting (with coloring and labels) OTUs at a threshold of at 80% ubiquity and greater than 1% relative abundance (represented by the red target). This threshold reveals the "core" taxa.

Corynebacterium, *Staphylococcus* and *Propionibacterium* emerge as the core taxa at both time points in the HV group and at the first visit in the EX group. The core taxa expanded by the second visit in the EX group to include, *Streptococcus* and *Bacillales* among others.
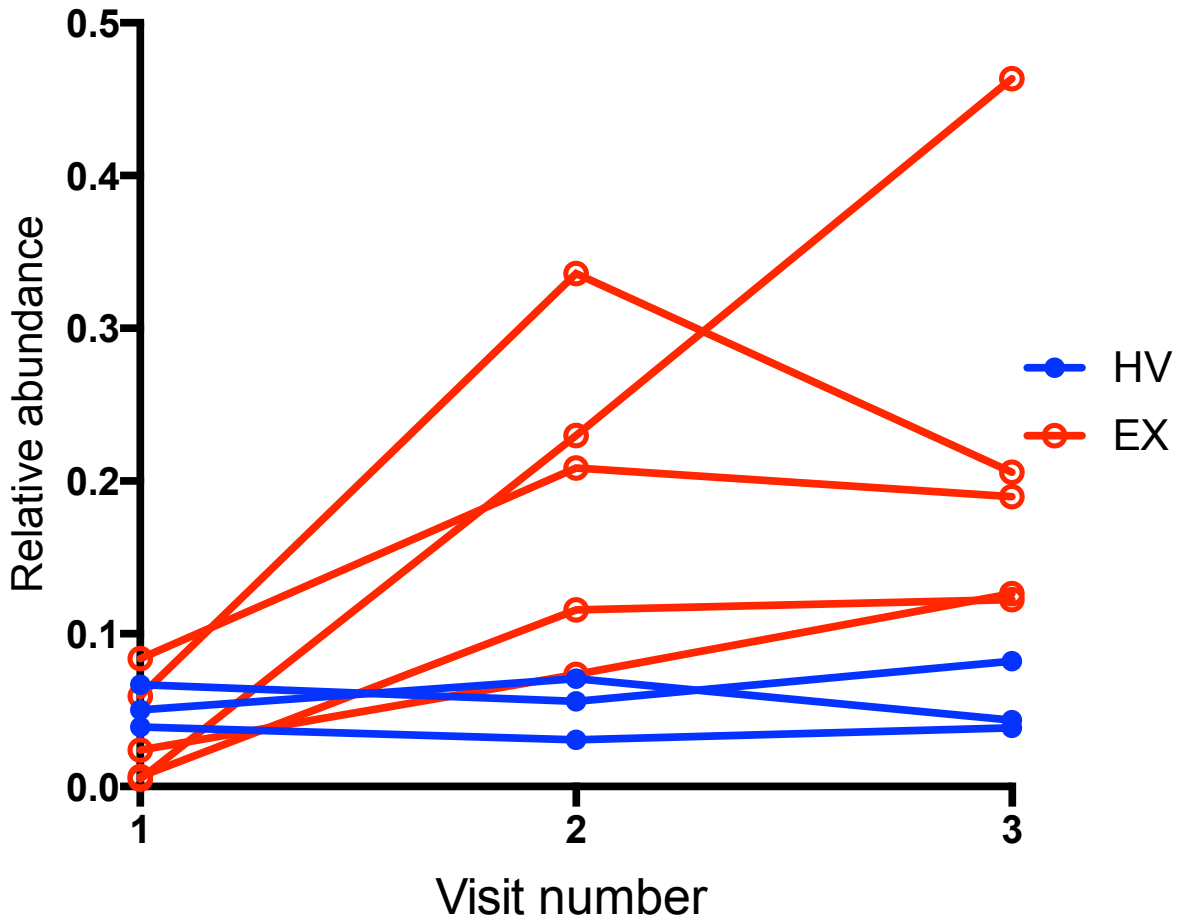
47

Figure S4: Graphic representation of the relative abundance of *Staphylococcus* over time in subjects classified as having a low baseline level of *Staphylococcus* (i.e., below 10%) at their first visit. The blue points represent the HV group while the red points represent members of the EX group.
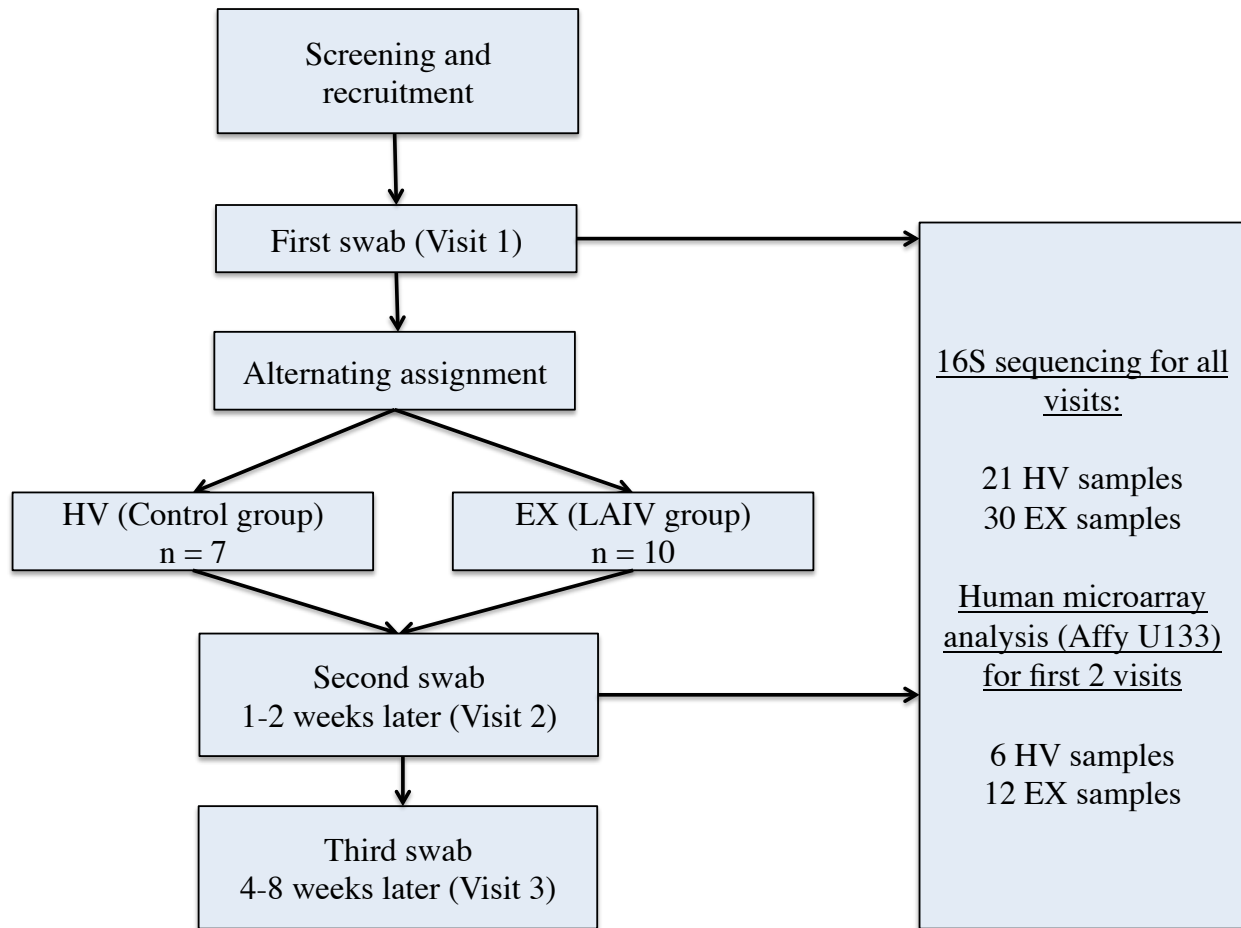
Figure S5: Flowchart of sampling procedures for subjects administered LAIV versus saline.
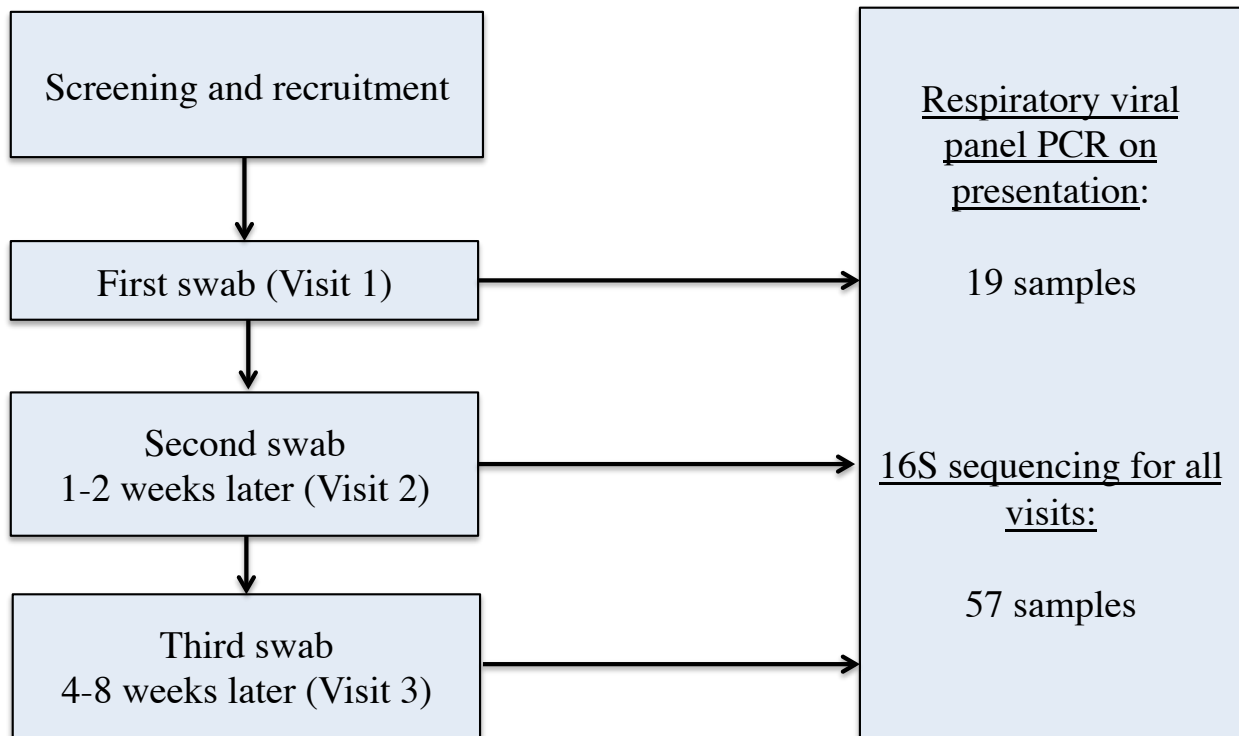
Figure S6. Flowchart of sampling procedures for subjects with flu-like illness.

Statistical Addendum: Compositional Data Transformation and Analysis:

Modeling or predicting compositional data is constrained by the fact that the predicted values should sum to a constant (in this case, 1). Any form of regression on the original relative values will violate this constraint. Transforming the relative abundances with a log-ratio transformation, however, no longer limits the outcome (y) to a set range (0 to 1). Unfortunately, while the modeling of transformed data is certainly feasible, the value and implications of the result based on the transformed data is more dubious. In this addendum, I will use the control group, which we have shown by PERMANOVA based on Bray-Curtis dissimilarities and comparisons of diversity not to be significantly changed between visits, to contrast two methods of analysis of compositional data over time. The data used for these comparisons are the genus level relative abundances for the HV group across the sequential visits.

Method 1: Paired comparisons of changes in relative abundance without transformation:
Paired Wilcox rank sum testing was applied to the relative abundances of all taxa between sequential visits and the results are ranked according to the resultant p-values. Al least the top 5 taxa are noted for each comparison, with more referenced when p-values were below 0.05 further down the ranked list. Absolute changes are noted for each case as well (in the form of first group minus second group).

Table A1: HV 2-1 without transformation

	p-value	difference
Peptoniphilus	0.016	-0.0061
Anaerococcus	0.14	-0.011
Clostridiales	0.14	-0.00021
Actinobacteria	0.16	-0.00049
Finegoldia	0.18	-0.0018

Table A2: HV 3-2 without transformation

	p-value	difference
Bacilli	0.031	0.020
Staphylococcaceae	0.031	0.0078
Gammaproteobacteria	0.036	-0.0015
Fusobacterium	0.059	0.037
Staphylococcus	0.078	0.12

Method 2: Paired comparisons of changes in relative abundance with additive log-ratio

transformation:

Prior to transformation, relative abundances of zero were replaced by the single lowest relative

abundance in the data set to avoid the natural log of zero. Next, OTUs were ordered by mean

relative abundance across all samples and the top 30 OTUs were isolated to be of interest,

while the remainder were summed together into the non-top 30 grouping. Zero values within the

latter group were once again replaced by the lowest value detected within the "non-top 30" set

to avoid division by zero.

Paired Wilcox rank sum testing was applied to the relative abundances of all taxa between

sequential visits and the results are ranked according to the resultant p-values. Al least the top 5

taxa are noted for each comparison. Absolute changes are noted for each case as well (in the

form of first group minus second group).

Table A3: HV 2-1 with ALR transformation

	p-value	differences
Neisseria	0.059	-1.67
Porphyromonas	0.20	-1.10
Veillonella	0.28	-1.32
Pseudomonas	0.31	-1.69
Actinomyces	0.31	-1.12

Table A4: HV 3-2 with ALR transformation

	p-value	differences
Aeromonas	0.059	1.45
Peptoniphilus	0.063	1.28
Neisseria	0.10	1.70
Propionibacterium	0.16	0.59
Anaerococcus	0.18	0.78

Comparison:

For each of the two differences (visit 2 – visit 1 and visit 3 – visit 2) the p-values from the top 30 comparisons of the transformed and non-transformed analyses were plotted on the same axes.

Figure A1: The distribution of p-values from the transformed and non-transformed analyses for the differences between visits 1 and 2.
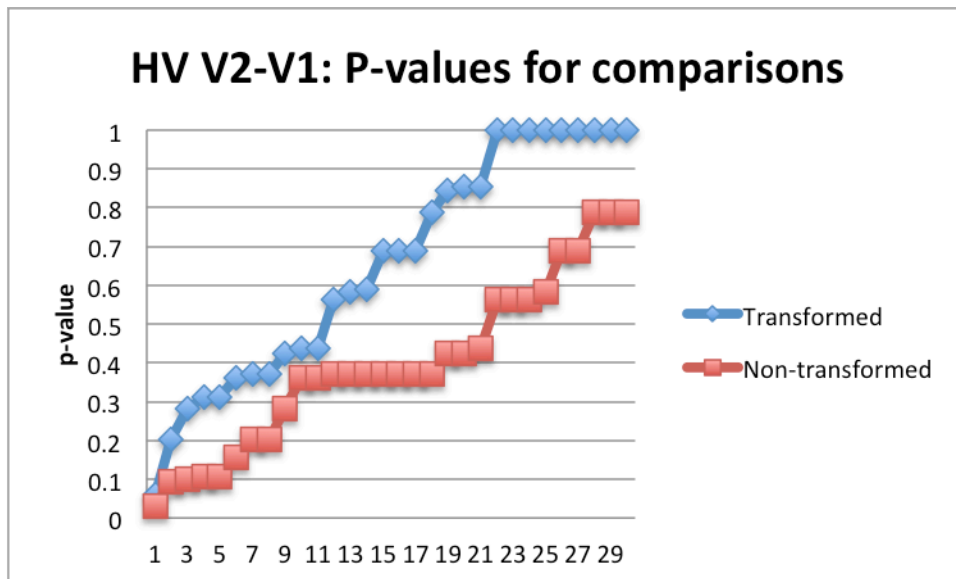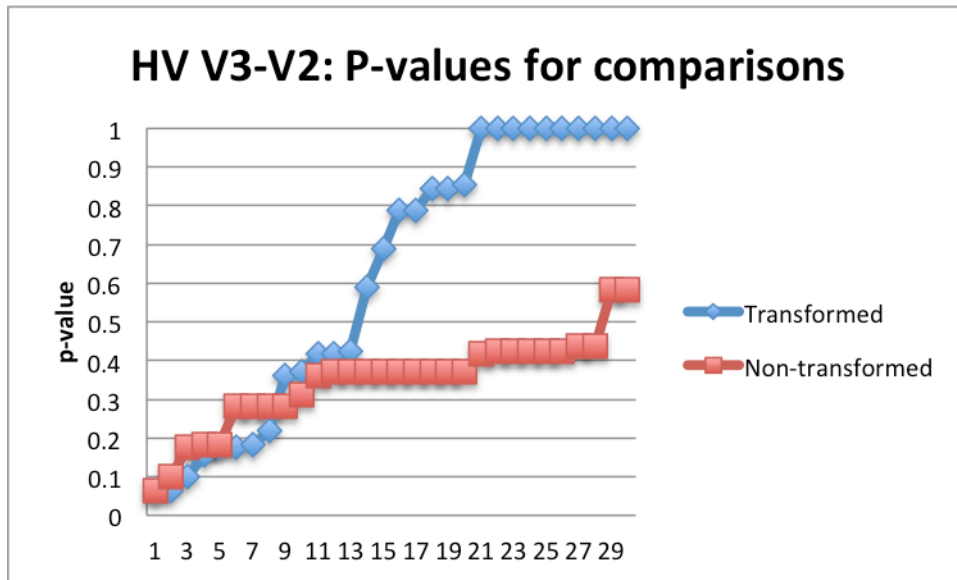
Figure A2: The distribution of p-values from the transformed and non-transformed analyses for the differences between visits 2 and 3.

Discussion:

Without correcting for multiple hypothesis testing, the ALR transformation appears skewed towards a p-value of 1, suggesting that the transformation may in fact be adding noise to the evaluation. Furthermore, the differences in ALR transformations are not meaningful on their own. The results are potentially more obscure as the transformation is limited by the necessary replacement of zero values with an arbitrary "low" number. Finally, the choice of the reference divisor is certainly arbitrary. In our case, the relative abundance of the non-top 30 was a relatively small value with much fluctuation (mean 0.039, standard deviation 0.036).

In conclusion, while comparisons of relative abundance are more meaningful, they are inherently limited. Unfortunately, while transformation of data can overcome these constraints, the results can be arbitrary and difficult to interpret. Alternative methods such as data mining based random forest designs should be entertained and validated for this particular problem.

References

1.   Schwarzmann SW, Adler JL, Sullivan Jr RJ, Marine WM. Bacterial pneumonia during the Hong Kong influenza epidemic of 1968-1969: experience in a city-county hospital. Archives of Internal Medicine. 1971;127(6):1037.

2.   Morens DM, Taubenberger JK, Fauci AS. Predominant role of bacterial pneumonia as a cause of death in pandemic influenza: implications for pandemic influenza preparedness. Journal of Infectious Diseases. 2008;198(7):962-70.

3.   Louie J, Jean C, Chen T, Park S, Ueki R, Harper T, et al. Bacterial coinfections in lung tissue specimens from fatal cases of 2009 pandemic influenza A (H1N1)-United States, May-August 2009. Morbidity and Mortality Weekly Report. 2009;58(38):1071-4.

4.   Johnson NP, Mueller J. Updating the accounts: global mortality of the 1918-1920" Spanish" influenza pandemic. Bulletin of the History of Medicine. 2002;76(1):105-15.

5.   Dawood FS, Iuliano AD, Reed C, Meltzer MI, Shay DK, Cheng P-Y, et al. Estimated global mortality associated with the first 12 months of 2009 pandemic influenza A H1N1 virus circulation: a modelling study. The Lancet infectious diseases. 2012;12(9):687-95.

6.   Rice TW, Rubinson L, Uyeki TM, Vaughn FL, John BB, Miller RR, 3rd, et al. Critical illness from 2009 pandemic influenza A virus and bacterial coinfection in the United States. Critical care medicine. 2012;40(5):1487-98.

7.   Hers J, Masurel N, Mulder J. Bacteriology and histopathology of the respiratory tract and lungs in fatal Asian influenza. The Lancet. 1958;272(7057):1141-3.

8.   Boutin S, Graeber SY, Weitnauer M, Panitz J, Stahl M, Clausznitzer D, et al. Comparison of Microbiomes from Different Niches of Upper and Lower Airways in Children and Adolescents with Cystic Fibrosis. PloS one. 2015;10(1):e0116029.

9.   Lozupone C, Cota-Gomez A, Palmer BE, Linderman DJ, Charlson ES, Sodergren E, et al. Widespread colonization of the lung by Tropheryma whipplei in HIV infection. American journal of respiratory and critical care medicine. 2013;187(10):1110-7.

10.   Sloan WT, Lunn M, Woodcock S, Head IM, Nee S, Curtis TP. Quantifying the roles of immigration and chance in shaping prokaryote community structure. Environmental microbiology. 2006;8(4):732-40.

11.   Charlson ES, Bittinger K, Haas AR, Fitzgerald AS, Frank I, Yadav A, et al. Topographical continuity of bacterial populations in the healthy human respiratory tract. Am J Respir Crit Care Med. 2011;184(8):957-63.

12.   Sze MA, Dimitriu PA, Hayashi S, Elliott WM, McDonough JE, Gosselink JV, et al. The lung tissue microbiome in chronic obstructive pulmonary disease. American journal of respiratory and critical care medicine. 2012;185(10):1073-80.

13.   Corbella X, Domíguez M, Pujol M, Ayats J, Sendra M, Pallares R, et al. Staphylococcus aureus nasal carriage as a marker for subsequent staphylococcal infections in intensive care unit patients. European Journal of Clinical Microbiology and Infectious Diseases. 1997;16(5):351-7.

14.   von Eiff C, Becker K, Machka K, Stammer H, Peters G. Nasal carriage as a source of Staphylococcus aureus bacteremia. New England Journal of Medicine. 2001;344(1):11-6.

15.   Corne P, Marchandin H, Jonquet O, Campos J, Banuls A-L. Molecular evidence that nasal carriage of Staphylococcus aureus plays a role in respiratory tract infections of critically ill patients. Journal of clinical microbiology. 2005;43(7):3491-3.

16.   Kluytmans J, Wertheim H. Nasal carriage of Staphylococcus aureus and prevention of nosocomial infections. Infection. 2005;33(1):3-8.

17.   Hageman JC, Uyeki TM, Francis JS, Jernigan DB, Wheeler JG, Bridges CB, et al. Severe community-acquired pneumonia due to Staphylococcus aureus, 2003–04 influenza season. Emerging infectious diseases. 2006;12(6):894-9.

18.   Nakamura S, Davis KM, Weiser JN. Synergistic stimulation of type I interferons during influenza virus coinfection promotes< i> Streptococcus pneumoniae</i> colonization in mice. The Journal of clinical investigation. 2011;121(9):3657-65.

19.   Sun K, Metzger DW. Inhibition of pulmonary antibacterial defense by interferon-γ during recovery from influenza infection. Nature medicine. 2008;14(5):558-64.

20.   Shahangian A, Chow EK, Tian X, Kang JR, Ghaffari A, Liu SY, et al. Type I IFNs mediate development of postinfluenza bacterial pneumonia in mice. The Journal of clinical investigation. 2009;119(7):1910.

21.   Trinchieri G. Type I interferon: friend or foe? The Journal of experimental medicine. 2010;207(10):2053-63.

22.   Furuya Y, Müllbacher A. Type I IFN Exhaustion is a Host Defence Protecting Against Secondary Bacterial Infections. Scandinavian journal of immunology. 2013;78(5):395-400.

23.   Metzger DW, Sun K. Immune Dysfunction and Bacterial Coinfections following Influenza. The Journal of Immunology. 2013;191(5):2047-52.

24.   Tripathi S, White MR, Hartshorn KL. The amazing innate immune response to influenza A virus infection. Innate immunity. 2013:1753425913508992.

25.   Yoo J-K, Kim TS, Hufford MM, Braciale TJ. Viral infection of the lung: Host response and sequelae. Journal of Allergy and Clinical Immunology. 2013;132(6):1263-76.

26.   Cox R, Brokstad K, Ogra P. Influenza virus: immunity and vaccination strategies. Comparison of the immune response to inactivated and live, attenuated influenza vaccines. Scandinavian journal of immunology. 2004;59(1):1-15.

27.   Wertheim HF, Menno van Kleef M, Vos MC, Ott A, Verbrugh HA, Fokkens W. Nose picking and nasal carriage of Staphylococcus aureus. Infection control and hospital epidemiology. 2006;27(8):863-7.

28.   Li K, Bihan M, Yooseph S, Methé BA. Analyses of the microbial diversity across the human microbiome. PloS one. 2012;7(6):e32118.

29.   Pawlowsky-Glahn VB, A. . Compositional data analysis: Theory and applications: John Wiley & Sons.; 2011.

30.   Kiser KB, Cantey-Kiser JM, Lee JC. Development and Characterization of a Staphylococcus aureus Nasal Colonization Model in Mice. Infection and immunity. 1999;67(10):5001-6.

31.   Tian X, Xu F, Lung WY, Meyerson C, Ghaffari AA, Cheng G, et al. Poly I: C enhances susceptibility to secondary pulmonary infections by gram-positive bacteria. PloS one. 2012;7(9):e41879.

32.   Chaban B, Albert A, Links MG, Gardy J, Tang P, Hill JE. Characterization of the Upper Respiratory Tract Microbiomes of Patients with Pandemic H1N1 Influenza. PloS one. 2013;8(7):e69559.

33.   Greninger AL, Chen EC, Sittler T, Scheinerman A, Roubinian N, Yu G, et al. A metagenomic analysis of pandemic influenza A (2009 H1N1) infection in patients from North America. PloS one. 2010;5(10):e13381.

34.   Yi H, Yong D, Lee K, Cho Y-J, Chun J. Profiling bacterial community in upper respiratory tracts. BMC infectious diseases. 2014;14(1):583.

35.   Allen EK, Koeppel AF, Hendley JO, Turner SD, Winther B, Sale MM. Characterization of the nasopharyngeal microbiota in health and during rhinovirus challenge. Microbiome. 2014;2(1):22.

36.   Mina MJ, McCullers JA, Klugman KP. Live attenuated influenza vaccine enhances colonization of Streptococcus pneumoniae and Staphylococcus aureus in mice. MBio. 2014;5(1):e01040-13.

37.   Palacios G, Hornig M, Cisterna D, Savji N, Bussetti AV, Kapoor V, et al. Streptococcus pneumoniae coinfection is correlated with the severity of H1N1 pandemic influenza. PloS one. 2009;4(12):e8540.

38.   Randolph AG, Vaughn F, Sullivan R, Rubinson L, Thompson BT, Yoon G, et al. Critically ill children during the 2009-2010 influenza pandemic in the United States. Pediatrics. 2011;128(6):e1450-8.

39.   Lemon KP, Klepac-Ceraj V, Schiffer HK, Brodie EL, Lynch SV, Kolter R. Comparative analyses of the bacterial microbiota of the human nostril and oropharynx. MBio. 2010;1(3).

40.   Yan M, Pamp SJ, Fukuyama J, Hwang PH, Cho D-Y, Holmes S, et al. Nasal Microenvironments and Interspecific Interactions Influence Nasal Microbiota Complexity and< i> S. aureus</i> Carriage. Cell host & microbe. 2013;14(6):631-40.

41.   Frank DN, Feazel LM, Bessesen MT, Price CS, Janoff EN, Pace NR. The human nasal microbiota and Staphylococcus aureus carriage. PloS one. 2010;5(5):e10598.

42.   Uehara Y, Nakama H, Agematsu K, Uchida M, Kawakami Y, Abdul Fattah A, et al. Bacterial interference among nasal inhabitants: eradication of Staphylococcus aureus from nasal cavities by artificial implantation of Corynebacterium sp. Journal of Hospital Infection. 2000;44(2):127-33.

43.   Mendelman PM, Cordova J, Cho I. Safety, efficacy and effectiveness of the influenza virus vaccine, trivalent, types A and B, live, cold-adapted (CAIV-T) in healthy children and healthy adults. Vaccine. 2001;19(17):2221-6.

44.   Barría MI, Garrido JL, Stein C, Scher E, Ge Y, Engel SM, et al. Localized mucosal response to intranasal live attenuated influenza vaccine in adults. Journal of Infectious Diseases. 2013;207(1):115-24.

45.   Cao RG, Suarez NM, Obermoser G, Lopez SM, Flano E, Mertz SE, et al. Differences in Antibody Responses between TIV and LAIV Influenza Vaccines Correlate with the Kinetics and Magnitude of Interferon Signaling in Children. Journal of Infectious Diseases. 2014:jiu079.

46.   Fischer II WA, Chason KD, Brighton M, Jaspers I. Live attenuated influenza vaccine strains elicit a greater innate immune response than antigenically-matched seasonal influenza viruses during infection of human nasal epithelial cell cultures. Vaccine. 2014;32(15):1761-7.

47.   Täubel M, Rintala H, Pitkäranta M, Paulin L, Laitinen S, Pekkanen J, et al. The occupant as a source of house dust bacteria. Journal of Allergy and Clinical Immunology. 2009;124(4):834-40. e47.

48.   Consortium HMP. A framework for human microbiome research. Nature. 2012;486(7402):215-21.

49.   Schloss PD, Westcott SL, Ryabin T, Hall JR, Hartmann M, Hollister EB, et al. Introducing mothur: open-source, platform-independent, community-supported software for describing and comparing microbial communities. Applied and environmental microbiology. 2009;75(23):7537-41.

50.   Corbata: CORe microBiome Analysis Tools. Available from: http://www.jcvi.org/cms/research/projects/corbata/overview/.

51.   Li K, Bihan M, Methé BA. Analyses of the stability and core taxonomic memberships of the human microbiome. PloS one. 2013;8(5):e63139.

52.   Heber S, Sick B. Quality assessment of Affymetrix GeneChip data. Omics: a journal of integrative biology. 2006;10(3):358-68.

53.   Bolstad BM, Irizarry RA, Astrand M, Speed TP. A comparison of normalization methods for high density oligonucleotide array data based on variance and bias. Bioinformatics. 2003;19(2):185-93.

54.   Irizarry RA, Bolstad BM, Collin F, Cope LM, Hobbs B, Speed TP. Summaries of Affymetrix GeneChip probe level data. Nucleic acids research. 2003;31(4):e15.

55.   Irizarry RA, Hobbs B, Collin F, Beazer-Barclay YD, Antonellis KJ, Scherf U, et al. Exploration, normalization, and summaries of high density oligonucleotide array probe level data. Biostatistics. 2003;4(2):249-64.

56.   Yaari G, Bolen CR, Thakar J, Kleinstein SH. Quantitative set analysis for gene expression: a method to quantify gene set differential expression including gene-gene correlations. Nucleic acids research. 2013;41(18):e170-e.

57.   Sanda C, Weitzel P, Tsukahara T, Schaley J, Edenberg HJ, Stephens MA, et al. Differential gene induction by type I and type II interferons and their combination. Journal of interferon & cytokine research. 2006;26(7):462-72.

58.   Falcon S, Gentleman R. Using GOstats to test gene lists for GO term association. Bioinformatics. 2007;23(2):257-8.